Chinese Journal of
POLYMER SCIENCE

REVIEW

https://doi.org/10.1007/s10118-026-3799-y
Chinese J. Polym. Sci.

Solid Polymer Electrolytes for Flexible Solid-State Batteries

Jia-Xin Li, Kun Zhang, Jia-Wei Zhao, Shi-Ze Gao, Chen Zhao, Bing-Jie Wang, Hui-Sheng Peng, and Meng Liao*

Department of Macromolecular Science, State Key Laboratory of Molecular Engineering of Polymers, Institute of Fiber Materials and Devices, and Laboratory of Advanced Materials, Fudan University, Shanghai 200438, China

Abstract As energy storage technologies move toward safer and mechanically adaptive formats, flexible solid-state batteries have become an important platform for powering next generation deformable systems. Solid polymer electrolytes (SPEs) are promising candidates for flexible solid-state batteries because their polymer-chain flexibility, film forming capability, and interfacial adaptability enable stable solid-solid electrode-electrolyte contact under low pressure or pressure free conditions. This review summarizes recent advances in SPEs for flexible solid-state batteries, covering linear polymers, topological polymer architectures, composite and multifunctional electrolytes, and representative fabrication strategies. Application oriented SPE designs are further discussed with a focus on material and device strategies for deformation adaptability, safety enhancement, and environmental adaptability. Finally, remaining challenges and future directions are outlined to guide the rational design of high performance SPEs for flexible energy storage.

Keywords Solid polymer electrolytes; Solid-state batteries; Flexible batteries; Functional polymer electrolytes

Citation: Li, J. X.; Zhang, K.; Zhao, J. W.; Gao, S. Z.; Zhao, C.; Wang, B. J.; Peng, H. S.; Liao, M. Solid polymer electrolytes for flexible solid-state batteries. *Chinese J. Polym. Sci.* https://doi.org/10.1007/s10118-026-3799-y

1 INTRODUCTION

Driven by the rapid expansion of mobile electronics, wearable healthcare, soft robotics, deformable sensors, and human machine interfaces, flexible solid-state batteries are emerging as important energy storage technologies that combine high safety, mechanical compliance, and stable electrochemical performance.[1–7] Their safety advantage mainly arises from replacing volatile and combustible organic liquid electrolytes with solid electrolytes, which can reduce the risks of electrolyte leakage, combustion, and thermally triggered failure.[8–11]

However, maintaining stable electrode–electrolyte contact across solid-solid interfaces remains a critical challenge. Inorganic solid electrolytes, such as oxide- and sulfide-based systems, typically rely on high external pressures (>50 MPa), often assisted by additional mechanical components (*e.g.*, springs or hydraulic devices), to ensure sufficient interfacial contact during battery operations, which is difficult to reconcile with the requirements of lightweight and deformable devices.[12–14] In this regard, SPEs provide a more suitable materials platform for flexible batteries. Their intrinsic polymer chain flexibility, film forming capability, and interfacial adaptability allow them to conform to electrode surfaces and maintain solid–solid contact under much lower pressure requirement (<5 MPa), enabling more stable electrode-electrolyte contact and ion transport under mechanical deformation. These features make SPEs more compatible with repeated bending, folding, twisting, and stretching, and position them as a key materials platform for flexible solid-state battery construction.[15,16]

The development of SPEs began with early salt polyether complexes and has gradually expanded toward more diverse polymer architectures aimed at balancing ion transport, interfacial stability, and mechanical robustness. Pioneering studies on poly(ethylene oxide) (PEO)-based systems established the fundamental concept of ion conduction through polymer media, while also revealing the strong coupling between ionic mobility and polymer segmental motion, as well as the conductivity limitations imposed by semi-crystallinity at ambient temperature.[17,18] Subsequent advances therefore moved beyond conventional linear PEO systems toward in-

* Corresponding author, E-mail: liaomeng@fudan.edu.cn
Invited Review
Received May 24, 2026; Accepted July 1, 2026; Published online August 28, 2026

creasingly complex polymer architectures and composite systems. More recently, the field has further shifted from simply maximizing ionic conductivity to a broader materials-design framework that also emphasizes decoupled ion transport, electrode-electrolyte interfacial regulation, mechanical resilience under deformation, manufacturability, and compatibility with high-energy electrodes.[19–21] This evolution has substantially expanded the role of SPEs from model ion-conducting media to multifunctional enabling materials for next-generation flexible solid-state batteries.

In this review, recent advances in SPEs for flexible solid-state batteries are discussed from three perspectives: materials design, synthesis/fabrication strategies, and practical scenario-oriented SPE design. Previous reviews have provided broad perspectives on polymer electrolytes for lithium batteries. This review further focuses on SPE design under flexible battery conditions, where flexibility, pressure free operation, and dynamic electrode-electrolyte contact introduce additional design criteria beyond electrochemical properties. The development of SPEs is first summarized in terms of linear polymer systems, topologically engineered polymer architectures, and composite SPEs containing functional fillers or secondary phases. Emphasis is placed on how polymer design evolves from improving ionic conductivity alone to simultaneously addressing mechanical robustness, deformation adaptability, and interfacial stability. Through this framework, the key structure-property relationships governing SPE performance under flexible operation are systematically discussed. Representative synthesis and fabrication strategies are then reviewed, with emphasis on how microstructure construction, interfacial engineering, and processing pathways influence electrolyte performance and electrode-electrolyte contact. Practical scenario-oriented SPE designs are further discussed, focusing on material and device strategies for deformation adaptability, safety enhancement, and environmental adaptability. Finally, the remaining scientific challenges and future directions are identified to guide the rational design of high performance SPEs for flexible energy storage applications.

2 POLYMER AND COMPOSITE DESIGN FOR SOLID POLYMER ELECTROLYTES

The key advantage of SPEs for flexible solid-state batteries arises from the intrinsic characteristics of polymers, including chain mobility, processability, and tunable interfacial interactions, which collectively enable deformable electrolytes with stable electrode-electrolyte contact and regulated ion transport. This section discusses SPEs from two perspectives: polymer architecture (covering linear or chain-like polymer systems and topologically engineered polymers) and composite design (covering composite polymer electrolytes containing functional fillers or secondary phases). Linear systems are presented as the basic platform for regulating Li^+ coordination and segmental dynamics through backbone and side chain design. Topological polymers further introduce structural freedom to organize ion conducting and mechanically reinforcing domains. Composite polymer electrolytes expand the design scope by integrating functional components to improve ion transport, mechanical robustness, and interfacial stability (Fig. 1 and Table 1).

2.1 Linear or Chain-like Polymer-based SPEs

The concept of SPEs can be traced to the seminal work of Peter V. Wright in 1973, who first demonstrated that alkali metal salts dissolved in PEO exhibit ionic conductivity.[17,22] In PEO/lithium salt systems, Li^+ coordinate with ether oxygen atoms along the polymer backbone and migrate *via* successive coordination and de-coordination processes assisted by segmental chain motion, establishing a characteristic coupling between ionic transport and polymer flexibility. Building on this foundational discovery, Michel Armand subsequently demonstrated the feasibility of PEO-based SPEs in lithium metal batteries, laying the groundwork for polymer-based solid-state electrochemistry.[23]

While PEO has played a foundational role in the development of SPEs, its practical performance under ambient conditions remains subject to certain intrinsic constraints. The relatively high crystallinity at room temperature limits segmental mobility, resulting in relatively low ionic conductivity (typically 10^{-6}–10^{-5} S·cm^{-1}). In addition, its mechanical strength and oxidative stability (about 3.8 V versus Li^+/Li) were insufficient to meet the requirements of high-voltage cathodes and mechanically demanding applications.[18,24] These considerations have motivated extensive efforts in the backbone engineering, aiming to regulate crystallinity, improve ion transport, and enhance overall electrochemical and mechanical performance. For example, polycarbonates (PCs) feature a high concentration of polar carbonate groups (—O—(C=O)—O—) along the backbone. The large dipole moment of these groups endows PCs with a high dielectric constant that facilitates salt dissociation, while their irregular molecular packing results in a predominantly amorphous structure, which provides continuous pathways for ion transport. Representative polypropylene carbonate-based electrolytes have achieved room-temperature conductivities on the order of 10^{-4} S·cm^{-1} with expanded electrochemical windows (about 4.5–4.6 V).[25] In addition, poly(ether-urethane) systems form microphase-separated morphologies arising from thermodynamic incompatibility between soft ether segments and hard urethane domains. Such hierarchical structures enable functional decoupling, where ion-conducting soft phases facilitate Li^+ transport *via* segmental motion, while hydrogen-bonded hard domains provide mechanical reinforcement and maintain structural integrity, thereby enabling a rare combination of high ionic conductivity (up to about 10^{-3} S·cm^{-1}) and robust mechanical strength (Fig. 2a).[26] Polysiloxane-based polymers, characterized by low rotational barriers (about 0.8 kJ·mol^{-1}) and ultralow glass transition temperatures (−120 °C), further illustrate the importance of backbone flexibility in promoting ion transport, although their weak coordination ability often requires compositional tuning.[27] Collectively, these systems highlight that polymer backbone chemistry plays a central role in determining the balance between segmental dynamics, ion coordination, and mechanical integrity, thereby influencing overall electrolyte performance.

Beyond backbone modification, side-chain engineering and functional group design provide additional routes to regulate ion transport and interfacial behavior. In particular, the introduction of highly polar moieties such as nitrile, carbonyl,

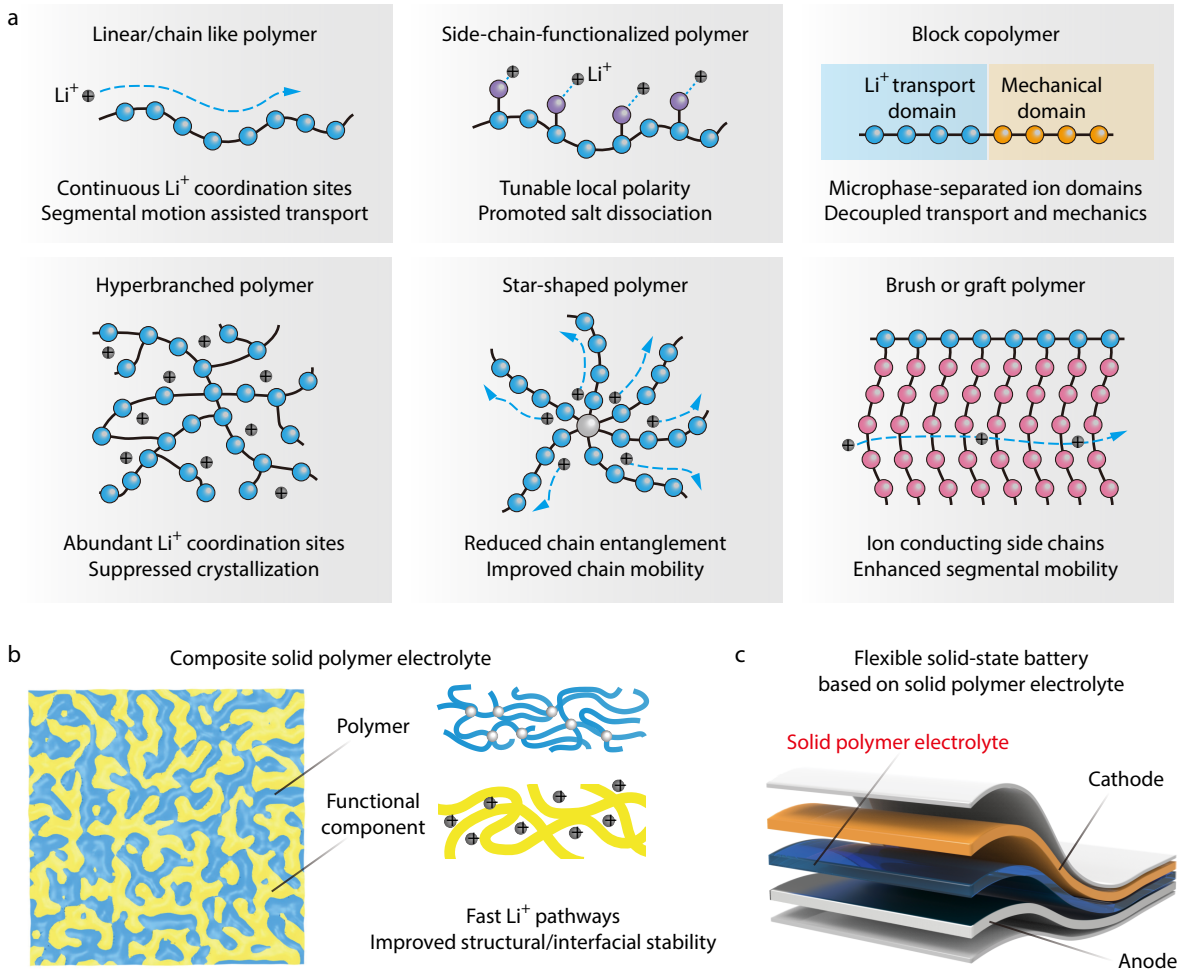

Fig. 1 (a) Representative polymer types and their roles in regulating Li^+ transport, salt dissociation, and mechanical properties in SPEs; (b) Composite SPEs with functional components for fast ion transport and improved stability; (c) Schematic of SPE-based, flexible solid-state battery.

and fluorinated groups can increase the local dielectric constant, facilitate lithium salt dissociation, and modulate Li^+ coordination environments.[28–35] These effects influence both bulk ion transport and interfacial chemistry, providing multiple handles for performance optimization. Different functional groups contribute in distinct yet complementary ways. For example, nitrile-containing polymers such as polyacrylonitrile (PAN) enable efficient ion solvation due to their strong polarity and high dielectric constant (about 30), while also improving thermal stability and promoting more stable interphases, thereby suppressing transition metal dissolution from high-energy cathodes (Figs. 2b and 2c).[28–30] Ester functional polymers such as poly(methyl methacrylate) provide high amorphous content and good interfacial compatibility with lithium metal, although their ion transport remains strongly coupled to segmental relaxation near the glass transition temperature.[31–33] In contrast, fluorinated polymers such as poly(vinylidene fluoride) (PVDF) provide wide electrochemical stability windows and strong electron withdrawing environments that are favorable for high voltage operation.[34] Because the semicrystalline nature of PVDF restricts segmental motion and limits ionic conductivity, copolymerization with hexafluoropropylene (HFP), as in PVDF-HFP, is often used to increase amorphous domains and enhance ion mobility.[35]

Taken together, the development of linear polymer based SPEs has expanded from classical PEO type matrices toward broader molecular design of ion conducting polymers. Backbone chemistry and side chain functionality provide complementary methods for regulating ion transport, mechanical response, and interfacial behavior within a unified polymer framework.

2.2 Topological Polymer-based SPEs

Building on the development of linear polymer electrolytes, recent efforts in molecular design have focused on regulating the relationship between polymer structure and ion transport. The intrinsic coupling between Li^+ migration and polymer segmental motion, together with the need for mechanical robustness and interfacial stability, has driven the exploration of more advanced polymer architectures for SPEs. In this context, topological polymers have emerged as a promising class of materials. Representative architectures such as block copolymers, hyperbranched polymers, star-shaped polymers, and comb or brush-like systems offer diverse routes toward multifunctional SPEs with balanced electrochemical and mechanical performance.[36–43] Compared with linear analogues, they typically exhibit higher densities of functional groups, reduced crystallinity, and lower glass transition temperatures, which facilitate lithium

https://doi.org/10.1007/s10118-026-3799-y

Table 1 Representative SPEs for flexible solid-state batteries discussed in this review.

Electrolyte composition	Ionic conductivity ($S·cm^{-1}$)	ESW [a] (V versus Li/Li^+)	Mechanical and flexibility features	Cell performance
PEO/LiTFSI[24] (linear polymer electrolyte)	2×10^{-5} at 30 °C	3.8	Tensile modulus of 10.5 MPa; tensile strain of 250%	Li||LFP: 90 $mAh·g^{-1}$ at 30 °C and 0.3 C
Poly(ether urethane)/LiTFSI[26] (linear polymer electrolyte)	1.1×10^{-3} at 25 °C	>4.3	Tensile strength 13 MPa; stretchable and bendable	Li||LFP: 99% capacity retention after 500 cycles at 0.5 C
PAN/PEO/LiTFSI[29] (linear polymer electrolyte)	10^{-5} to 10^{-4} at 60 °C	/	Tensile strength 50 MPa; elongation at break ≈26%	Li||LFP: stable cycling for 100 cycles at 2 C and 150 °C
PVDF-HFP/LiTFSI[35] (linear polymer electrolyte)	1.21×10^{-4} at 25 °C	5.15	Tensile strength 2.2 MPa; elongation at break 250%	Li||LFP: 98.65% capacity retention after 100 cycles at 0.2 C and 25 °C
PBC-mb-PBS copolymer/LiTFSI[37] (block polymer electrolyte)	6.20×10^{-5} at 30 °C	4.48	Tensile strength 176.5 MPa; elongation at break 94.8%	Li||LFP: 85.7% capacity retention after 900 cycles at 0.2 C; pouch cell could operate under bending, cutting, or puncture
HPU/LiTFSI[38] (hyperbranched polymer electrolyte)	4.0×10^{-4} at 25 °C	4.95	Tensile strength 0.5 MPa; elongation at break ≈150%	Li||LFP: 83% capacity retention after 1000 cycles at 0.5 C; pouch cell remains operational under bending
PS-*b*-PLA-*b*-MeOPEG/PEO/LiTFSI[39] (star-shaped polymer electrolyte)	4.56×10^{-4} at 70 °C	4.28	Tensile strength 8.7 MPa; elongation at break 1315%; superior deformability without fracture	Li||LFP: 96% capacity retention after 300 cycles at 70 °C
PDMS-*g*-P(TFEA-*b*-PEGA)/LiTFSI[43] (brush-like polymer electrolyte)	1.8×10^{-4} at 30 °C	5.23	Soft and free standing	Li||LFP: 96% capacity retention after 200 cycles at 0.2 C and 30 °C
PVDF/CN@LLZTO/LiTFSI[53] (composite polymer electrolyte)	7.56×10^{-4} at 30 °C	4.90	Tensile strength 20.01 MPa; elongation at break 170.9%	Li||NCM811: 88.22% retention after 150 cycles at 0.5 C; bendable pouch cells
PEO/PA-$Li_{0.3}Cd_{0.85}PS_3$/LiTFSI[54] (composite polymer electrolyte)	1.02×10^{-2} at 25 °C	5.0	Young's modulus 2.2 GPa; tensile strain up to 330%; effective under pressure-less conditions (<0.1 MPa)	Li||NCM811: 92% retention after 600 cycles at 0.2 $mA·cm^{-2}$ under a stack pressure <0.5 MPa
PEO/ SMP(G4/SbF_3)/LiTFSI[55] (composite polymer electrolyte)	2.4×10^{-4} at 25 °C	4.5	Young's modulus 8.04 MPa; yield strength 0.43 MPa	Li||LFP: 91.7% capacity retention after 600 cycles at 1.0 C; pouch cell durable of bending, nail penetration, and cutting
PEO/MBO-550/LiTFSI[56] (composite polymer electrolyte)	2.7×10^{-4} at 50 °C	5.08	Tensile strength 4.13 MPa; Young's modulus 1.84 MPa	Li||LFP: 88.9% after 200 cycles at 0.1 C and 30 °C; foldable pouch cell
PBA/SN/LiTFSI[62] (composite polymer electrolyte)	1.1×10^{-3} at 20 °C	4.75	Elongation at break ~300%; adhesion energy 21.5 $J·m^{-2}$	Li||LFP: 99.5% capacity retention after 1000 cycles at 1 C
PVEC/UiO-66-FV/LiTFSI/LiDFOB[65] (composite polymer electrolyte)	6.78×10^{-4} at 30 °C	4.8	Young's modulus of 19.6 MPa	Li||LCO: 77.0% capacity retention after 200 cycles at 0.5 C

[a] Electrochemical stability window.

salt dissociation and ion mobility. At the same time, their structural versatility provides additional degrees of freedom for tuning ion transport, mechanical properties, and interfacial behavior.[44,45]

Block copolymer-based electrolytes, composed of chemically distinct polymer segments covalently linked together, can self-assemble into ordered microphase-separated nanostructures, in which ion-conductive and mechanically reinforcing domains coexist in a continuous framework.[36] As a representative example, a rigid–flexible coupled multiblock copolymer was developed *via* molecular design, consisting of a crystalline polybutylene succinate (PBS) phase and a polar cyano-functionalized phase, polydibutyl 2-(2-cyanoethyl)malonate (PBC).[37] The PBS domains served as physical crosslinking points that improved tensile strength (176.5 MPa) and low temperature toughness, while the highly polar PBC domains facilitated lithium salt dissociation and Li^+ transport. In addition, the formation of a Li_3N-rich interfacial layer improved oxidative stability and compatibility with high-voltage cathodes. By tuning the block ratio, a series of microphase-separated structures were obtained, enabling balanced optimization of ionic conductivity and mechanical properties. The optimized electrolyte exhibited ionic conductivities of 6.20×10^{-5} $S·cm^{-1}$ at 30 °C and 4.22×10^{-4} $S·cm^{-1}$ at 60 °C. After compositing with polyethylene, the bi-continuous structure further enhanced mechanical strength and enabled uniform lithium deposition at high current densities. The resultant Li||$LiNi_{0.83}Co_{0.05}Mn_{0.12}O_2$ (NCM-83) cell delivered a capacity retention of 82.9% after 100 cycles at 1.0 C, demonstrating the potential of such multiblock copolymer electrolytes for high-voltage applications.

Hyperbranched polymers and star-shaped polymers further extend the design space through three-dimensional architectures. Hyperbranched polymers, characterized by densely distributed branching points, could suppress the crystallization and introduce abundant coordination sites for Li^+, thereby enhancing ionic conductivity and interfacial compatibility. As a typical example, a hyperbranched polyurethane electrolyte was synthesized by reacting hyperbranched poly(ethylene glycol) (HPEG) with isophorone diisocyanate (IPDI) (Fig. 3a).[38] Benefiting from the hyperbranched structure and the plasticizing effect of ionic liquids, the system exhibited enhanced lithium salt dissociation, electrochemical stability, and Li^+ mobility. Meanwhile, the involved hydrogen bonding interactions induced microphase separation and facilitated the formation of ion transport pathways, while also improving interfacial contact and stabilizing electrode-electrolyte interphases. These advantages enabled the

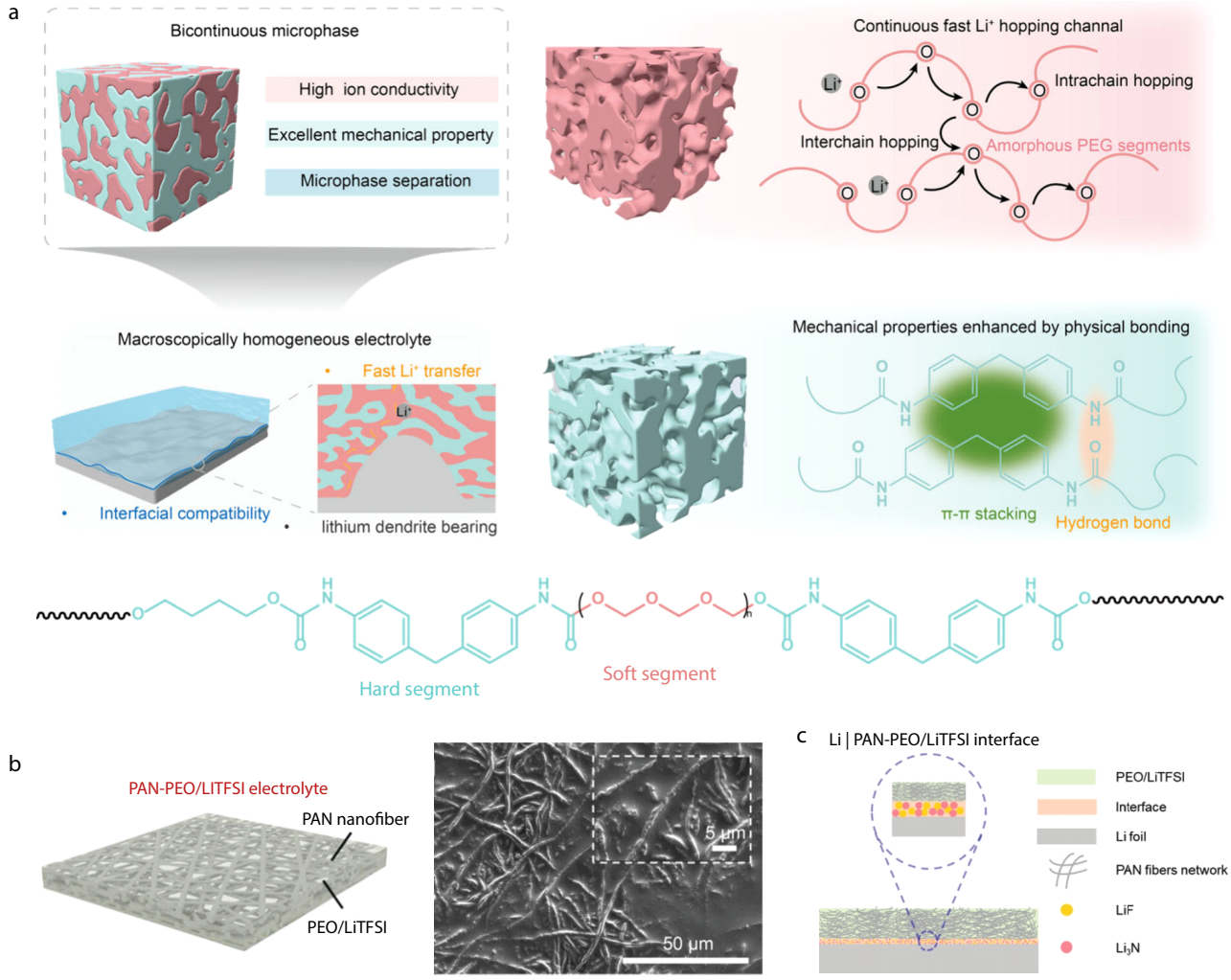

Fig. 2 (a) Schematic of microphase-designed linear poly(ether-urethane) SPEs (Reproduced with permission from Ref. [26]; Copyright (2025), American Chemical Society); (b) Schematic illustration of PAN-PEO/LiTFSI electrolyte and SEM image of PAN-PEO/LiTFSI electrolyte from top view (inset shows a typical magnified SEM image of panel); (c) Schematic illustration for Li|PAN-PEO/LiTFSI interface (b, c: reproduced with permission from Ref. [29]; Copyright (2022), Wiley-VCH).

assembled Li||$LiFePO_4$ (LFP) cell to deliver a discharge capacity of 118 mAh·g^{-1} after 1000 cycles at 0.5 C at room temperature. Along the same design principle, polymer entropy regulation offers another effective strategy.[39,40] Star-shaped polymers, composed of multiple linear chains connected to a central core, can reduce chain entanglement and increase conformational freedom, thereby promoting more dynamic and less crystalline ion conducting structures. One representative example is an ABC-type star-shaped terpolymer prepared by atom transfer radical polymerization, ring opening polymerization, and click chemistry, which forms a high entropy microphase interlocked polymer electrolyte and self assembles into a dynamic interpenetrating polymer network after blending with PEO and lithium salt (Fig. 3b).[39] This structure enhanced mechanical strength, suppressed crystallinity, and restricted anion migration, leading to an improved Li^+ transference number of 0.63 and excellent thermal stability (T_d >400 °C) (Fig. 3c). The corresponding Li||LFP cell exhibited 96% capacity retention after 300 cycles at 70 °C.

Comb-like and brush-like polymer-based electrolytes provide another important structural strategy by spatially separating ion-conductive side chains from the backbone. In comb-like systems, side chains are relatively sparse and can adopt random coil conformations, whereas in bottlebrush polymers, high grafting density results in extended cylindrical architectures.[41] Early studies demonstrated that comb-like polysiloxanes bearing oligo(ethylene oxide) side chains, synthesized from poly(methylhydrosiloxane) precursors, could achieve ionic conductivities approaching 10^{-4} S·cm^{-1} at room temperature when complexed with $LiClO_4$ (EO/Li^+ of about 25).[42] Although crosslinking or blending with high-molecular-weight PEO may reduce conductivity to some extent, it significantly improved mechanical properties and enabled flexible film formation. More recently, bottlebrush polymer electrolytes have attracted increasing attention because their densely grafted side chains reduce chain entanglement, increase local free volume, and promote continuous Li^+ transport pathways. For example, a block-brush polymer electrolyte termed "ion-conductive wires" was constructed by grafting fluorinated–polyethylene glycol block copolymer

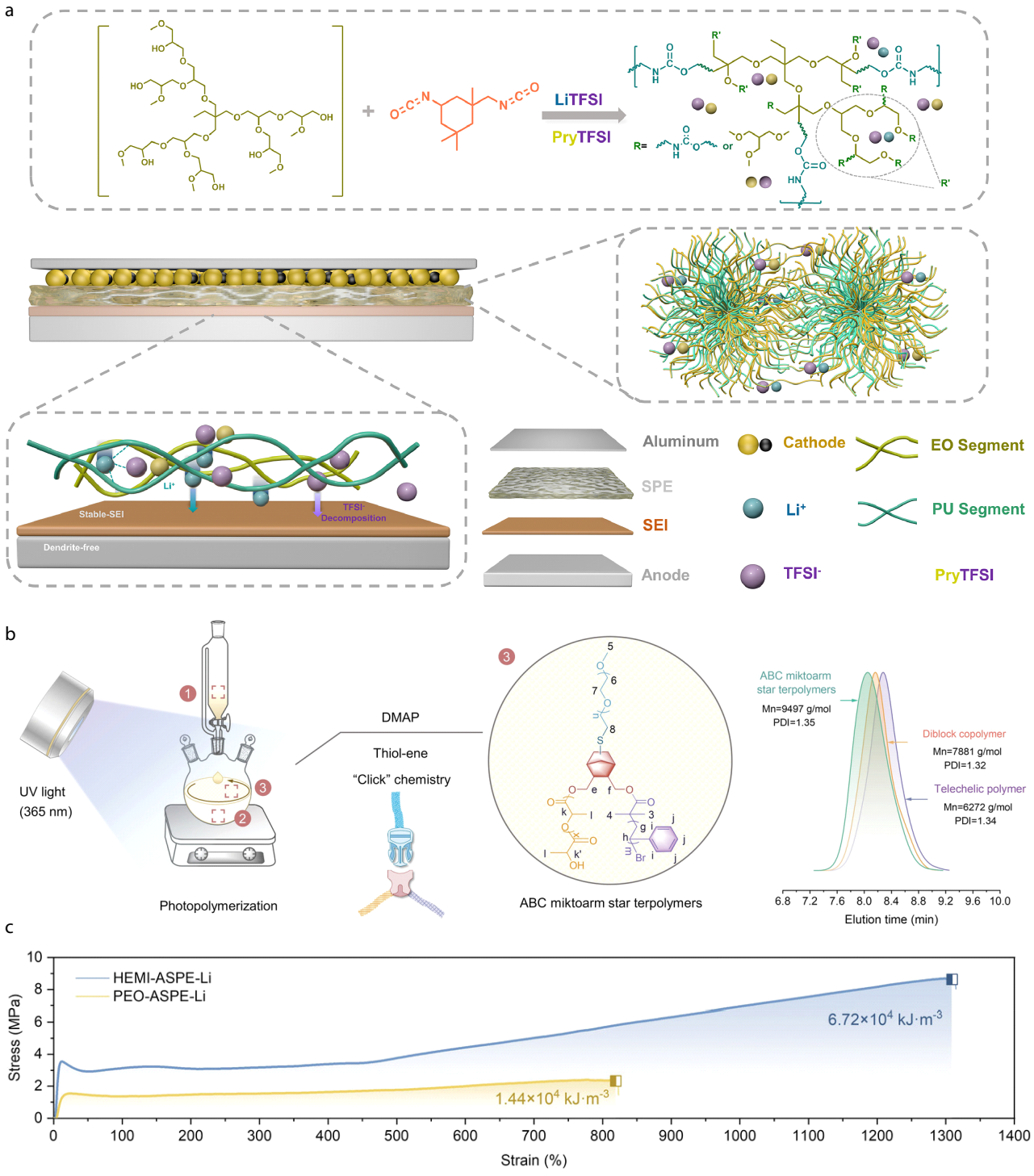

Fig. 3 (a) Schematic of hyperbranched polyurethane based electrolyte and assembled lithium-ion battery (Reproduced with permission from Ref. [38]; Copyright (2024), Elsevier); (b) Synthetic of the ABC miktoarm star terpolymers (ABCTPs) *via* click chemistry with the molecular formula of product (3, ABCTPs) inserted and the corresponding gel permeation chromatography test results; (c) Extension comparison of the star-shaped high-entropy microdomain interlocking all-solid-state polymer electrolyte with LiTFSI (HEMI-ASPE-Li) and PEO-ASPE-Li membranes (b, c: reproduced with permission from Ref. [39]; Copyright (2023), Wiley-VCH).

side chains, synthesized *via* reversible addition-fragmentation chain transfer polymerization, onto a polysiloxane backbone through thiol–ene click chemistry.[43] This architecture formed a core–shell structure, in which the poly(ethylene glycol) (PEG)-rich core facilitates Li^+ transport and the fluorinated shell enhances oxidative stability, suppressing anion migration and stabilizing the solid electrolyte interphase (SEI). Notably, without incorporating liquid components or inor-

ganic fillers, the electrolyte achieved an ionic conductivity of 1.8×10^{-4} S·cm^{-1}, a Li^+ transference number of 0.62, and an oxidation stability up to 5.23 V at 30 °C. The corresponding Li||LFP batteries showed stable cycling (capacity retention >96% over 200 cycles at 0.2 C), indicating the potential of brush-like topological structures for next generation solid state electrolytes.

2.3 Composite Polymer-based SPEs

Compared with single component polymer design, the incorporation of functional components into polymer matrices offers a more versatile route to regulate electrolyte properties. By integrating complementary functionalities from different material systems without substantially increasing synthetic complexity, composite strategies enable simultaneous enhancement of ionic conductivity, mechanical robustness, and interfacial stability, making them an important direction toward practical SPEs.[46–49]

Composite solid electrolytes based on inorganic fillers and polymer matrices represent one of the most established strategies in this category. Inorganic solid electrolytes, including oxides, sulfides, and halides, offer high ionic conductivity, wide electrochemical stability windows, and high mechanical modulus, but their brittleness, limited flexibility, and poor interfacial wettability restrict direct use in flexible batteries.[50] Polymer matrices, by contrast, provide mechanical compliance and intimate electrode-electrolyte contact. The integration of inorganic fillers into polymer matrices therefore enables composite solid electrolytes combined with inorganic phase derived ion transport and mechanical reinforcement from polymer-based flexibility and interfacial compatibility.[51,52] For instance, Wang *et al.* developed a composite electrolyte by coating porous 2D graphitic carbon nitride (g-C_3N_4) onto $Li_{6.4}La_3Zr_{1.4}Ta_{0.6}O_{12}$ (LLZTO) nanoparticles and dispersing the hybrid fillers within a PVDF matrix.[53] The strong metal nitrogen interactions between LLZTO and g-C_3N_4 facilitated continuous Li^+ transport pathways and promoted the formation of a Li_3N-rich SEI, which suppressed side reactions between the electrolyte and lithium metal. Benefiting from the enhanced Li^+ kinetics, the resulting composite exhibited a high ionic conductivity of 7.56×10^{-4} S·cm^{-1} and Li^+ transference number of 0.49, while maintaining stable cycling performance. Beyond interfacial coupling between nanoparticles and polymer matrices, constructing ordered inorganic ion conducting frameworks offers a more direct route to decouple ion transport from mechanical flexibility. Along this direction, Lan *et al.* designed a layered composite electrolyte composed of vertically aligned two-dimensional $Li_xM_yPS_3$ (M=Cd/Mn) nanosheets alternately stacked with PEO (Figs. 4a

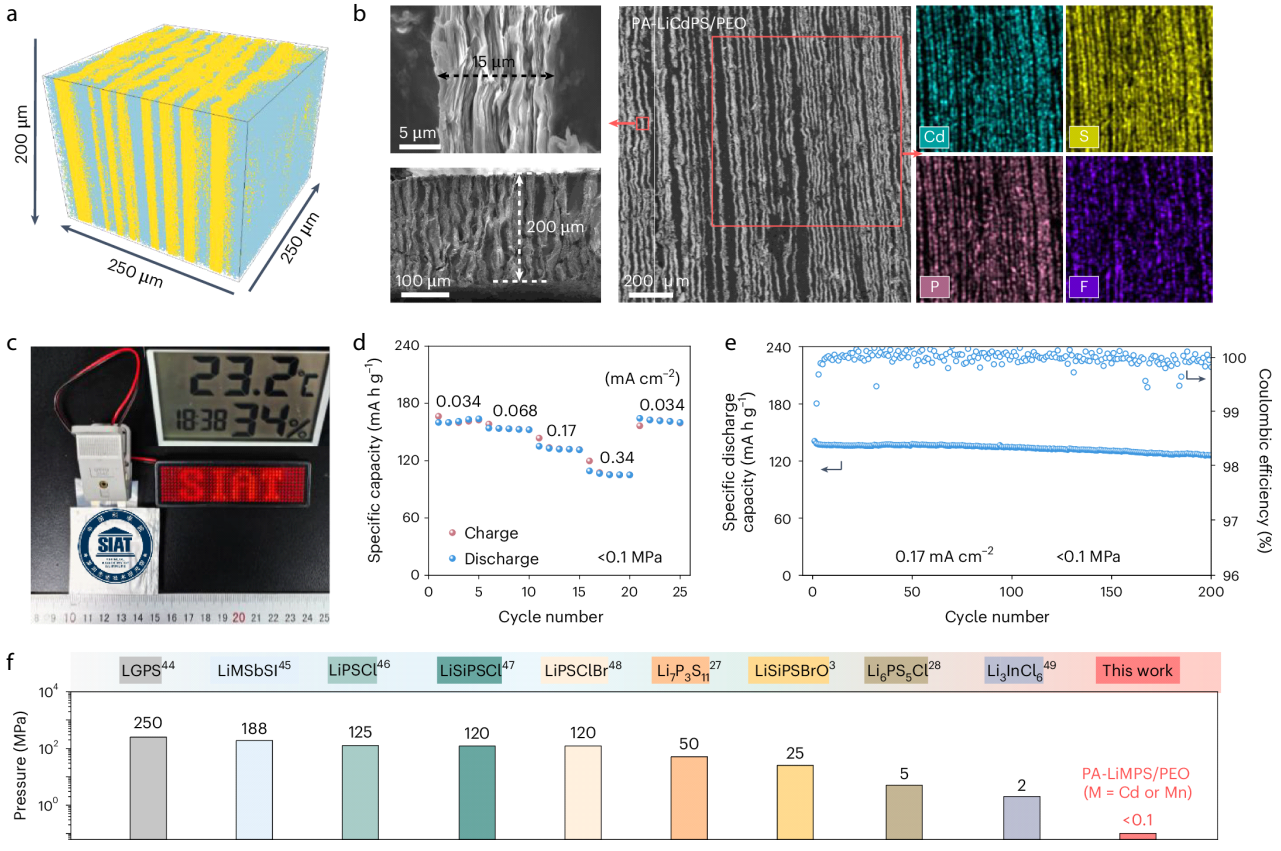

Fig. 4 (a) 3D TOF-SIMS image of the PA-$Li_{0.3}Cd_{0.85}PS_3$/PEO electrolyte; (b) High magnification surface SEM image, cross-sectional SEM image and low-magnification surface SEM image with corresponding elemental maps of the PA-$Li_{0.3}Cd_{0.85}PS_3$/PEO electrolyte; (c) Optical image of LEDs powered by a Li||LFP pouch cell; (d) Rate capability and (e) cycling performance of the pressure-less (*i.e.*, <0.1 MPa) Li||LFP pouch cells at 0.17 mA·cm^{-2} and within 2.5–3.9 V; (f) Comparison of the stack pressures needed by using previously reported electrolytes with high ionic conductivities and the PA-LiMPS/PEO electrolyte (M=Cd or Mn). (Reproduced with permission from Ref. [54]; Copyright (2025), Springer Nature.)

and 4b).[54] The vertically aligned nanosheets provided continuous superionic-conducting channels, while the PEO layers imparted flexibility, enabling effective decoupling of ionic transport and mechanical properties. The resulting composite solid electrolyte comprising perpendicularly aligned $Li_{0.3}Cd_{0.85}PS_3$ nanosheets in a PEO matrix (PA-$Li_{0.3}Cd_{0.85}PS_3$/PEO) achieved an ultrahigh ionic conductivity of 10.2 mS·cm^{-1} at room temperature and demonstrated stable cycling under low or negligible pressure (Figs. 4c–4f).

Molecular plasticizers have also been increasingly used to regulate polymer electrolyte properties, with recent efforts focusing on functional designs that improve ionic conductivity without sacrificing mechanical strength. Shen *et al.* introduced a supramolecular plasticizer (SMP) based on halogen bonding between tetraglyme (G4) and SbF_3.[55] When incorporated into PEO matrices, the SMP enhanced chain mobility and formed dynamic crosslinking interactions, leading to an ionic conductivity of 2.4×10^{-4} S·cm^{-1} and a tensile strength of 8.1 MPa at 25 °C. In addition, the electrolyte induced an inorganic-rich SEI that enabled stable lithium deposition, and pouch cells could operate under bending, puncturing, and cutting conditions. Similarly, Ren *et al.* developed a multi-arm boron-containing oligomer (MBO) as a solid plasticizer for PEO-based electrolytes.[56] The Lewis acidic boron sites interacted with anions to promote amorphous salt cluster formation and facilitated Li^+ transport, while the methoxy-terminated polyethylene glycol arms provided compatibility and physical crosslinking (Figs. 5a and 5b). By melt-infiltrating the SPE into a porous polyimide (PI) membrane using a solvent-free hot-pressing technique, an integrated cathode was constructed (Figs. 5c and 5d). The assembled high-loading Li||LFP pouch cell achieved an average discharge capacity of 152.4 mAh·g^{-1} over the first 100 cycles at 0.1 C, with a capacity retention superior to that of previously reported all-solid-state

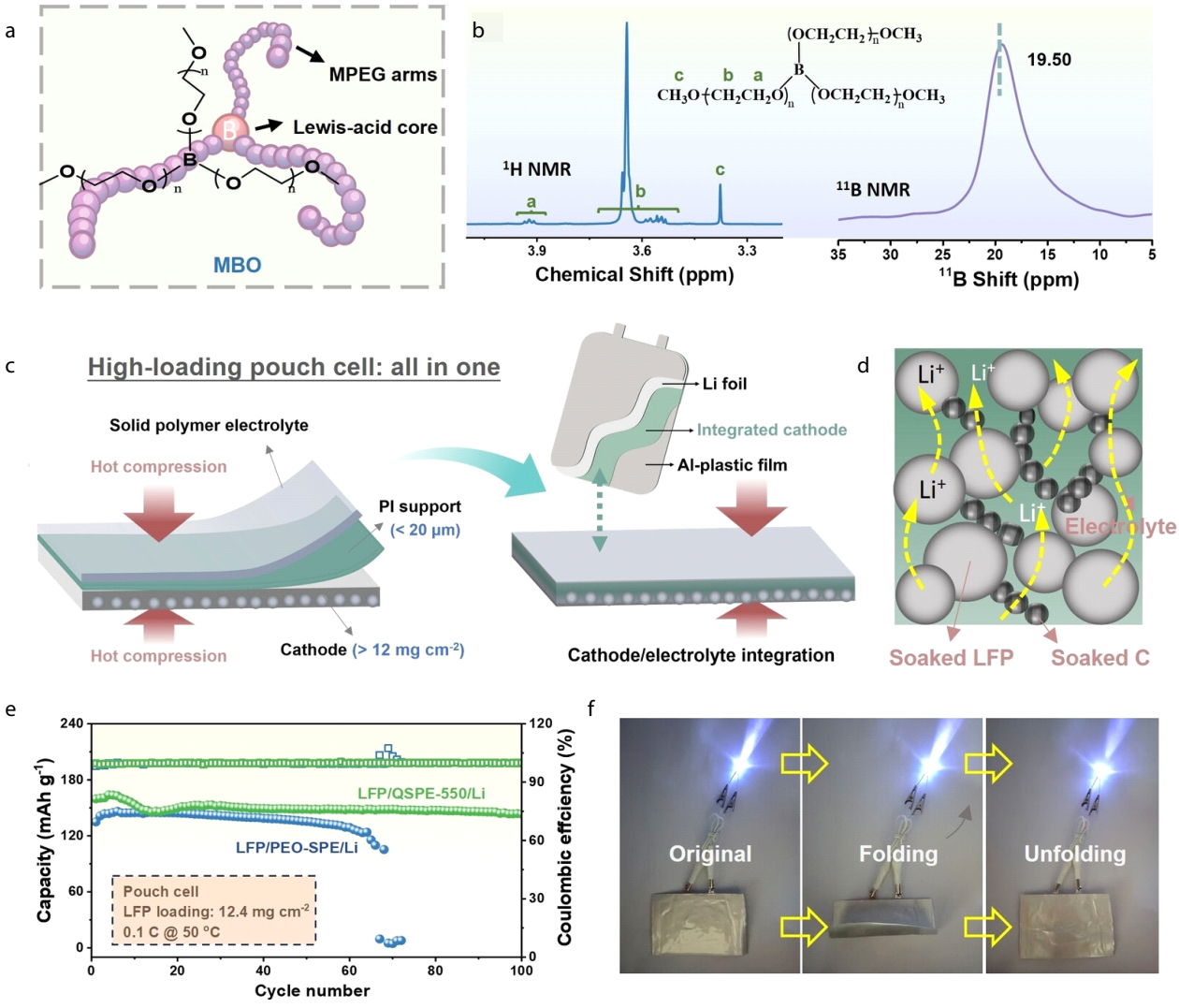

Fig. 5 (a) The chemical structure of the designed MBO plasticizer for composite polymer solid-state electrolytes; (b) The ^{1}H-NMR and ^{11}B-NMR spectra of MBO; (c) Schematic diagram of the preparation route of integrated LFP cathode and all-in-one Li||LFP pouch cell; (d) Internal structure of the integrated cathode with high LFP mass loading; (e) Cycling performance of all-solid-state Li||LFP pouch cells under 0.1 C at 50 °C; (f) Digital photos of a Li||LFP pouch cell based on the supramolecularly reinforced cross-linked polymer electrolyte with MBO-550 solid plasticizer lighting a light-emitting diode. (Reproduced with permission from Ref. [56]; Copyright (2025), Wiley-VCH.)

batteries (Fig. 5e). Moreover, the cell enabled stable operations even under bending and flattening conditions, demonstrating excellent cycling stability, mechanical toughness, and safety (Fig. 5f).

In addition to oligomeric solid plasticizers, plastic crystalline succinonitrile (SN) has been widely explored because of its strong affinity for Li^+ and its ability to regulate solvation structures.[57–60] The two nitrile groups in SN effectively extract Li^+ from polymer matrices, thereby enhancing ionic transport while promoting the formation of stable, inorganic-rich SEI layers. For example, a poly(methyl methacrylate-*co*-methacrylamide)/SN solid electrolyte was developed, simultaneously achieving a high toughness (24.8 $MJ·m^{-3}$), an ionic conductivity of 2.8 $mS·cm^{-1}$ at 25 °C, and a Li^+ transference number of 0.76.[61] When paired with a $LiNi_{0.6}Co_{0.2}Mn_{0.2}O_2$ cathode at 4.3 V, the resulting batteries maintained 90 % capacity retention after 500 cycles, demonstrating excellent long-term stability. Lee *et al.* further incorporated SN into a poly(butyl acrylate) elastomer matrix to construct a plastic crystal elastomer electrolyte (PCEE) with a three-dimensional interconnected conductive network (Fig. 6a).[62] This unique architecture enabled continuous ion-transport pathways while preserving mechanical elasticity. The resulting PCEE achieved an ionic conductivity of 1.1 $mS·cm^{-1}$ at 20 °C, a Li^+ transference number of 0.75, and low interfacial resistance. Moreover, the Li||NCM-83 cell with a low N/P ratio of 3.4 still maintained a capacity of 1.1 $mAh·cm^{-2}$ after 100 cycles at 30 °C and 0.5 $mA·cm^{-2}$ (Fig. 6b). Even at a high current density of 1 $mA·cm^{-2}$, the cell retained a capacity of 1.3 $mAh·cm^{-2}$, demonstrating excellent rate capability (Fig. 6c).

Metal organic frameworks (MOF), with well-defined pores, tunable coordination environments, and abundant Lewis acidic sites, provide an effective platform for promoting lithium salt dissociation, regulating ion transport pathways, and suppressing polymer crystallization in composite polymer electrolytes.[63] Hong *et al.* reported a MOF-808/PEO composite electrolyte, in which MOF-808 particles enhanced ion transport and extended the electrochemical stability window to 4.8 V, achieving an ionic conductivity of 9.7×10^{-4} $S·cm^{-1}$ at 60 °C, about 20 times higher than that of pure PEO.[64] More recently, Deng *et al.* proposed a self-crosslinked MOF–polymer electrolyte by functionalizing UiO-66 with the polymerizable vinyl and fluorinated groups, followed by *in situ* polymerization with a poly(vinylene ethylene carbonate) (PVEC) ma-

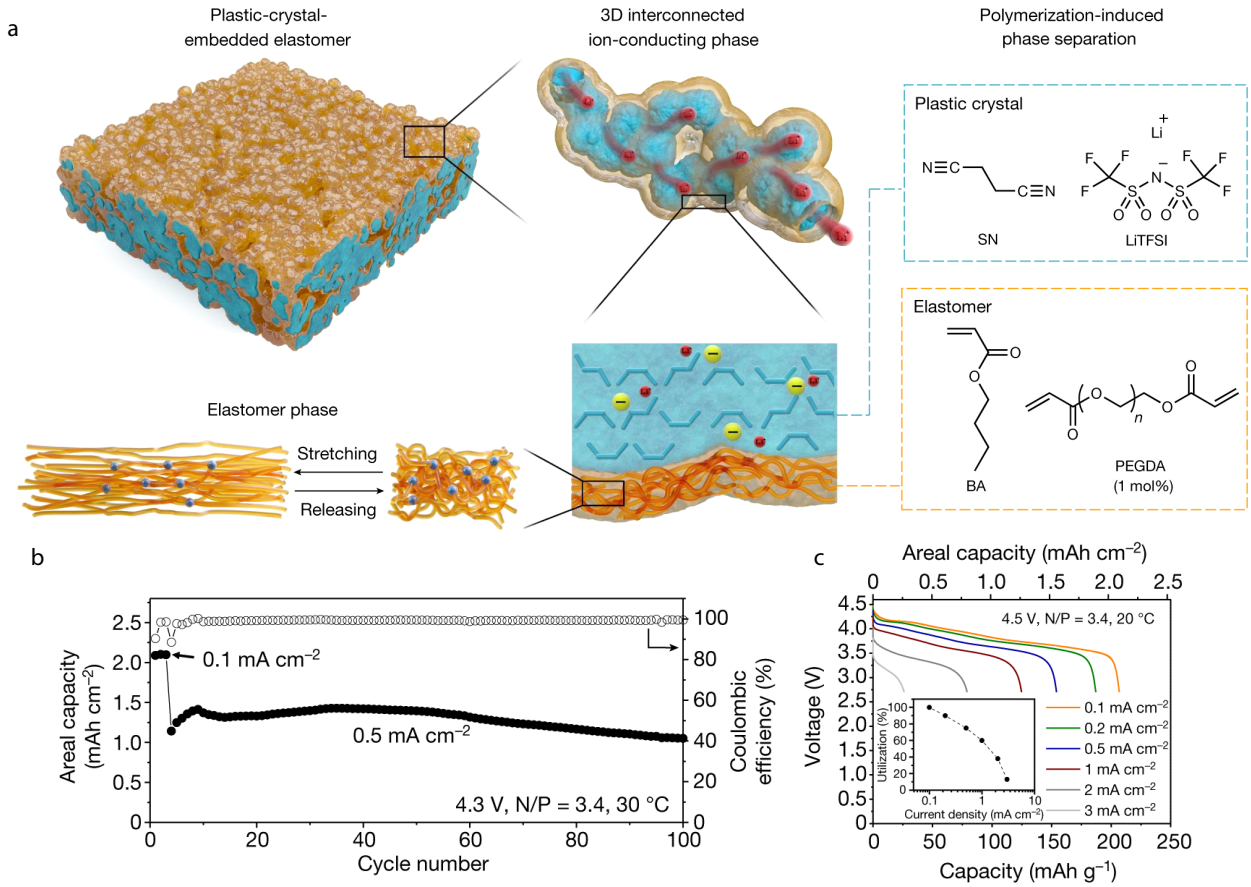

Fig. 6 (a) Schematic illustration of the design and structure for PCEE. The structure of PCEE shows that the 3D interconnected plastic crystal phase (cyan) is surrounded by the elastomer phase (orange). The plastic crystal phase supports a fast ion-conducting pathway, whereas the elastomer phase provides superior mechanical extensibility; (b) Cycling performance of the full cell as a function of cycle number in the voltage range of 2.7–4.3 V. The cell was initially cycled at a current density of 0.1 $mA·cm^{-2}$ for 3 cycles before cycling at 0.5 $mA·cm^{-2}$; (c) Rate capability of the full cell in the voltage range of 2.7–4.5 V at equal current densities. Inset: the capacity utilization at different areal current densities. (Reproduced with permission from Ref. [62]; Copyright (2022), Springer Nature.)

trix.[65] This molecular-level integration improved interfacial compatibility and structural stability, resulting in an ionic conductivity of 0.68 mS·cm^{-1} at room temperature, a Li^+ transference number of 0.76, and an electrochemical stability window up to 4.8 V. The corresponding Li symmetric cells remained stable for over 1400 h, while Li||$LiCoO_2$ (LCO) cells retained 77.0% capacity after 200 cycles at 0.5 C, highlighting MOF based composite design as an effective strategy for improving ion transport, mechanical integrity, and long-term interfacial stability in SPEs.

Overall, polymer and composite design determines SPE performance through coupled structure dynamic interface relationships rather than through a single material parameter. In linear polymers, Li^+ transport is governed by the balance between coordination strength and segmental relaxation, where glass transition temperature, crystallinity, dielectric environment, and functional group polarity jointly determine the density and mobility of Li^+ hopping sites. Topological polymers provide additional control over this balance by regulating chain packing, entanglement, microphase separation, physical crosslinking, and free volume, thereby decoupling ion conducting domains from mechanically reinforcing domains to different extents. Composite SPEs further introduce polymer filler and polymer plasticizer interactions, which can modify local solvation structures, suppress crystallization, redistribute mechanical stress, and stabilize electrode electrolyte interfaces. These relationships indicate that SPE design for flexible solid-state batteries should not be limited to increasing ionic conductivity, but should rationally coordinate Li^+ coordination dynamics, segmental mobility, modulus, toughness, adhesion, and interfacial stability under coupled electrochemical and mechanical operation.

3 SYNTHESIS AND FABRICATION STRATEGIES OF SOLID POLYMER ELECTROLYTES

Beyond materials design, fabrication and integration strategies are equally important for realizing high performance flexible solid-state batteries. The processing route determines electrolyte thickness, microstructure, and electrode-electrolyte contact, which in turn affects ion transport, mechanical adaptability, and device-level energy density.[66] Based on the electrolyte formation process, these strategies can be classified into ex situ construction and *in situ* polymerization.

3.1 *Ex situ* Synthesis and Fabrication Methods

Thus far, ex situ fabrication represents the primary approach for polymer electrolytes based on PEO, PVDF, and PAN, owing to its mature processing protocols, broad materials compatibility, and good control over membrane thickness and composition, allowing preformed polymer systems to be processed into well controlled membranes before cell assembly. Accordingly, ex situ membrane forming techniques have been widely developed, with wet processing methods such as solution casting, blade coating, electrophoretic deposition, and electrospinning being the most mature and versatile due to their compositional tunability and structural controllability.[67–71] Zhang *et al.* demonstrated solution casting for a PVDF/LLZTO composite electrolyte, achieving an ionic conductivity of about 5×10^{-4} S·cm^{-1} at 25 °C, Young's modulus of 30.8 MPa, and thermal stability up to 310 °C.[69] To improve processing efficiency and interfacial integration, Yao *et al.* developed a rapid electrophoretic deposition (EPD) method to deposit an ultrathin (20–50 μm) $Li_{1.3}Al_{0.3}Ti_{1.7}(PO_4)_3$ (LATP)/PEO/lithium bis(trifluoromethanesulfonyl)imide (LiTFSI) electrolyte layer directly onto LFP cathodes, reducing fabrication time from hours to minutes and enabling 85% capacity retention after >350 cycles at 45 °C (Figs. 7a and 7b).[70] Along this direction, Zheng *et al.* employed coaxial electrospinning and fabricated a three dimensional PVDF/SiO_2/$Li_{0.33}La_{0.557}TiO_3$ core shell fibrous electrolyte, which delivered an ionic conductivity of 1.26×10^{-4} S·cm^{-1}, a tensile strength of 46.8 MPa, and stable Li||Li cells cycling over 400 h.[71]

Although wet processing methods offer high versatility, the involvement of solvents may affect membrane quality and interfacial stability through pore formation during evaporation, residual solvent traces, or local compositional inhomogeneity.[72] Solvent-free dry processing has therefore attracted increasing attention as a complementary strategy, in which polymer and filler components are consolidated through thermal or mechanical methods. By eliminating solvent evaporation and drying steps, dry processing can reduce energy consumption, improve material utilization, and avoid solvent residue induced defects. This capability was demonstrated by hot pressing dynamic covalent polyimine with sulfide ceramic powders at 100 °C and 228 MPa to fabricate a composite electrolyte.[73] The reversible imine bonds endowed the polymer with sufficient flowability during processing, allowing it to fill interparticle voids and form a dense inorganic continuous and polymer filled structure. The resulting electrolyte exhibited an ionic conductivity of 0.092 mS·cm^{-1} at room temperature. Extending this solvent free processing strategy, Zhao *et al.* reported a solvent-free hot-pressed electrolyte that combines high mechanical strength of 161 MPa with an ionic conductivity of 4.42×10^{-4} S·cm^{-1}, enabling stable Na plating and stripping in sodium symmetric cells for over 2500 h.[74]

To further improve structural complexity and device integration, advanced manufacturing techniques such as 3D printing have also been introduced, providing new opportunities to fabricate polymer electrolytes with programmable architectures and precise spatial control.[75] In this regard, Han *et al.* first demonstrated the fully 3D-printed (3DP) all-solid-state sodium-ion battery by incorporating $BiFeO_3$ (BFO) nanofibers into a PEO-based electrolyte. The resulting 3DP-$Na_3V_2(PO_4)_3$||3DP-PEO-5BFO-$NaClO_4$||3DP-(hard carbon) cell achieved stable long-term cycling at 0.1 C and room temperature, retaining a discharge capacity of 42.7 mAh·g^{-1} with a capacity retention of 62.2% after 80 cycles.[76] Yang *et al.* further combined 3D printing with dynamic covalent chemistry to fabricate integrated cathode-electrolyte structures based on furan functionalized PEG and maleimide modified LLZTO (Figs. 7c and 7d).[77] This approach enabled Li||LFP cells to achieve stable cycling over 30000 cycles at 10 C with a capacity retention of 41.02%, and more importantly, shifted electrolyte fabrication from conventional membrane preparation toward architecture- and interface-level design.

3.2 *In situ* Synthesis and Fabrication Methods

In contrast to preformed membranes, *in situ* polymerization introduces liquid precursors into electrode structures, followed by polymerization inside the cell. This strategy enables conformal

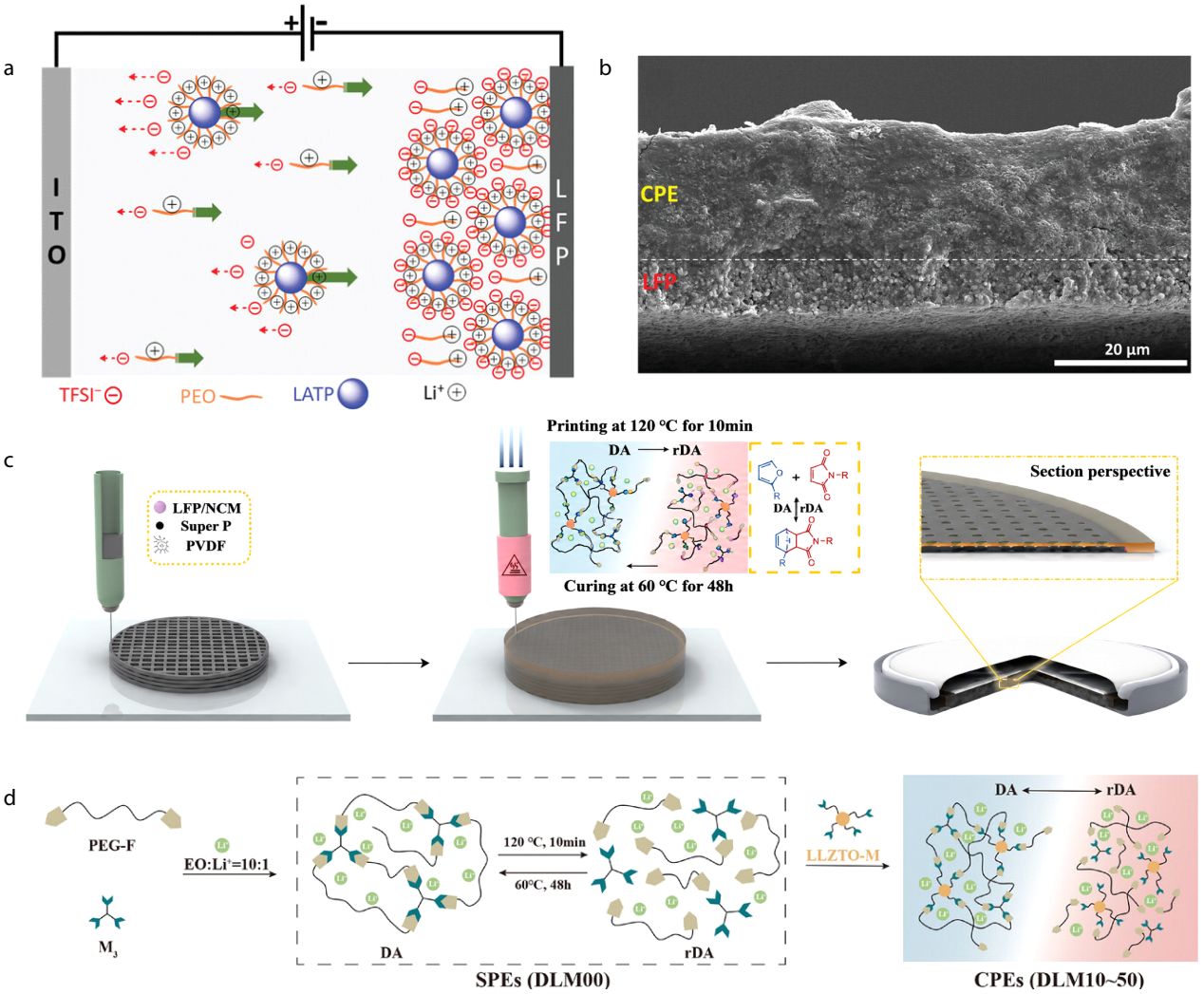

Fig. 7 (a) Schematic illustration for the EPD preparation of composite-polymer electrolyte; (b) Cross-sectional SEM image of LFP cathode and EPD-CPE70 (electrophoretically deposited composite polymer electrolyte with 70 wt% LATP) (a, b: reproduced with permission from Ref. [70]; Copyright (2023), Wiley-VCH); (c) Schematic fabrication process of the *in situ* 3D-printed integrated porous cathode/electrolyte architecture based on the thermally reversible Diels-Alder (DA) bonds; (d) Schematic illustration of the composite polymer electrolytes with covalent adaptable networks *via* thermally reversible DA reaction (c, d: reproduced with permission from Ref. [77]; Copyright (2025), Wiley-VCH).

electrode-electrolyte contact, reduces electrolyte thickness, shortens ion transport pathways, and lowers interfacial resistance, thereby improving device-level energy density.[78] Depending on the initiation mechanism, *in situ* polymerization can be mainly categorized into thermal, photo, and electrochemical initiation.

Among these strategies, thermally initiated polymerization is one of the most widely used approaches because of its broad monomer compatibility and suitability for solvent free systems, including ring opening polymerization and double bond radical polymerization.[79] As an early example of thermally triggered ring opening chemistry, Nair *et al.* reported a lithium salt catalyzed cationic ring opening polymerization of poly(ethylene glycol) diglycidyl ether using a $LiBF_4$/LiTFSI dual salt system, enabling polymerization at 80 °C within 1 h.[80] The resulting electrolyte exhibited an ionic conductivity of 0.113 mS·cm^{-1} and an electrochemical window above 5.5 V. Building on the similar thermal initiation principle, Huang *et al.* extended this strategy to fluoropolyether based radical polymerization, wherein the fluorinated chemistry promoted anion-rich solvation structures and fluorine-rich interphases, enabling long-term stable cycling and excellent rate capability in lithium-rich manganese-based layered oxide (LRMO)||Li cells, while the anode-free pouch cell further achieved a high energy density of 604 Wh·kg^{-1} (Figs. 8a–8c).[81]

Compared with thermal initiation, photo initiation provides milder reaction conditions and more precise spatial control, making it particularly suitable for constructing thin electrolyte layers on electrodes.[82] Along this line, He *et al.* used UV curing to fabricate an ultrathin electrolyte of approximately 10 μm (Fig. 8d).[83] Mechanical simulation tests demonstrated that the mechanical strength of the SPE-filled LFP cathode was significantly enhanced, with no damaged regions observed under an applied strain of 0.05 (Fig. 8e). More recently, electrochemical initiation has further shifted polymerization from externally triggered processing to cell inter-

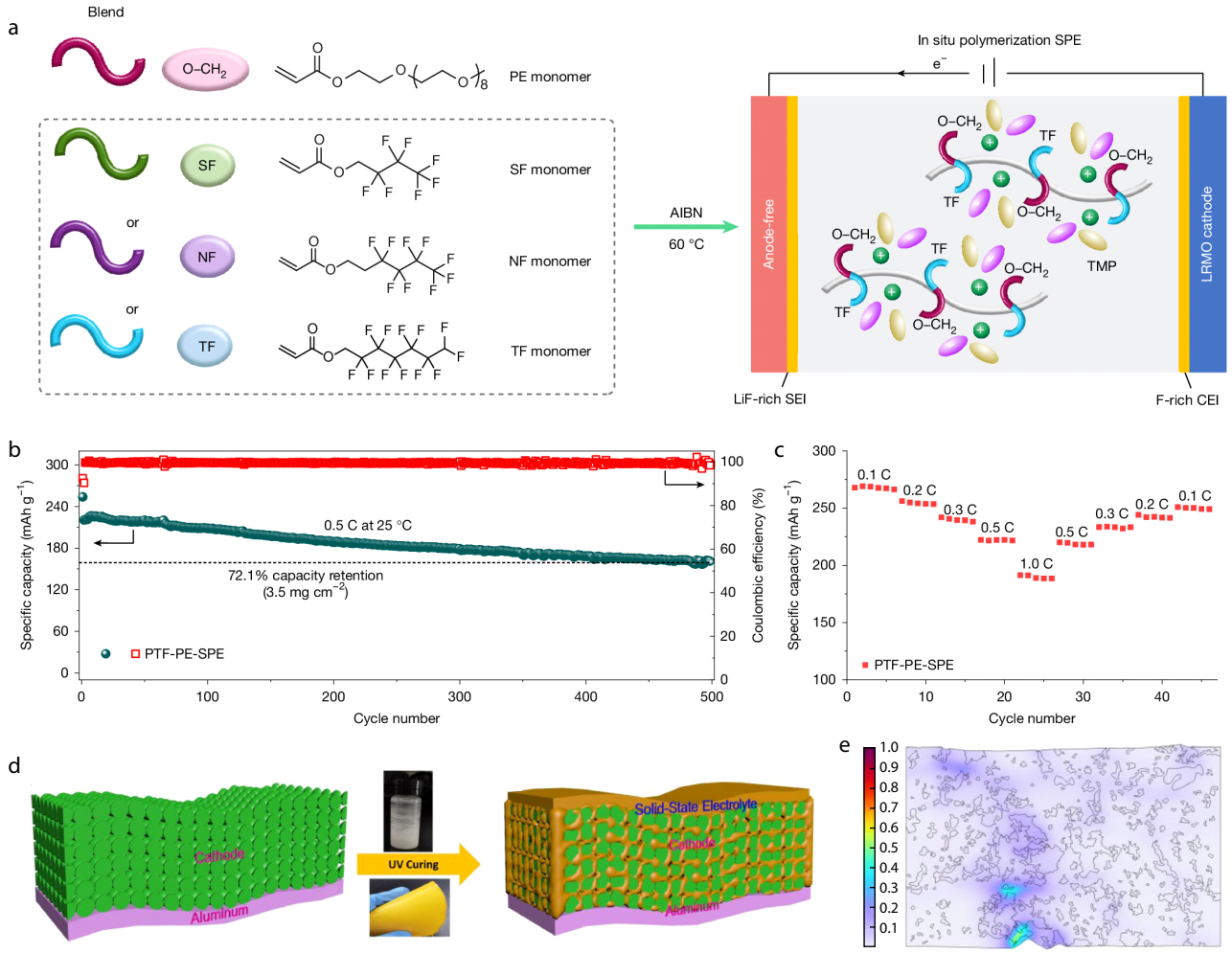

Fig. 8 (a) Schematic of synthesizing of fluoropolyether copolymers through *in situ* polymerization catalysed by 2,2′-azobis(2-methylpropionitrile) (AIBN); (b) The long-term cycling of Li||LRMO cells using poly(dodecafluorooctyl acrylate-*co*-poly(ethylene glycol) methyl ether acrylate) solid polymer electrolyte (PTF-PE-SPE) at 0.5 C; (c) Rate performance of Li||LRMO cells using PTF-PE-SPE at 25 °C (a–c: reproduced with permission from Ref. [81]; Copyright (2025), Springer Nature); (d) Preparation of cathode filled with composite solid-state electrolytes through UV-curing process; (e) A cathode filled with solid-state electrolytes remains intact at the same strain of 0.05 (Reproduced with permission from Ref. [83]; Copyright (2023), Elsevier).

nal self-activation, where electrochemical reactions directly initiate polymer formation during battery operation. For example, Zhu *et al.* demonstrated an electrochemically induced polymerization process triggered at 4.2 V, which generated gradient polymer structures and stable interfaces.[84] The resulting electrolyte exhibited an ionic conductivity of 0.56 mS·cm^{-1} and enabled Li||LFP cells to retain 88.9% capacity after 740 cycles at 0.5 C.

4 SOLID POLYMER ELECTROLYTE DESIGN TOWARDS FLEXIBLE BATTERIES

Beyond satisfying the fundamental electrochemical requirements of electrolytes, such as ionic conductivity, electrochemical stability, mechanical robustness, and interfacial compatibility, SPEs for flexible solid-state batteries should also be designed according to practical application scenarios. In flexible and wearable devices, the electrolyte is expected to maintain stable ion transport and electrode-electrolyte contact under bending, twisting, stretching, and pressure-free operation, while ensuring safety under mechanical or thermal abuse and reliable performance across variable environmental conditions.[85] Therefore, the design of SPEs is increasingly moving from materials-level optimization toward device-level integration. In this section, application-oriented design strategies are discussed from three aspects, deformation adaptability, safety, and environmental adaptability.

4.1 Deformation Adaptability-oriented Design of SPEs

Practical flexible batteries are expected to operate under bending, stretching, twisting, and pressure free conditions, where stable electrode-electrolyte contact becomes as important as bulk ionic conductivity.[86] Mechanical deformation can induce contact loss, local delamination, and increased interfacial resistance, leading to performance decay. Therefore, maintaining interfacial integrity and structural adaptability under realistic operating conditions has become an important design considera-

tion for SPEs.[87] In this context, high adhesion is first needed to preserve electrode-electrolyte contact under pressure free operation, while adaptive mechanical response enables the electrolyte to accommodate continuous deformation. Since repeated bending, stretching, and cycling can still generate cracks or interfacial defects, self-healing capability further provides a route to repair accumulated damage and extend device lifetime.

Interfacial adhesion provides a direct route to stabilize electrode-electrolyte contact under pressure free operation. By suppressing interfacial separation, strong adhesion helps maintain continuous ion transport pathways and further stabilize local electrochemical reactions at the interface. Along this direction, a high entropy polymer tape electrolyte with a soft-rigid gradient nanophase structure was constructed through Li bond interactions.[88] This design combined interfacial adhesion with mechanical reinforcement, delivering an ionic conductivity of 0.24 mS·cm^{-1} at room temperature, a tensile strength of about 22.1 MPa, a toughness of 87.7 MJ·m^{-3}, and an elastic recovery rate of 66.7%. Its adhesion strength was comparable to that of commercial adhesive tapes, enabling stable battery operation without external pressure (Fig. 9a). Beyond macroscopic contact stabilization, adhesion also governs lithium deposition at the microscopic level. Specifically, Li *et al.* designed a highly adhesive polymer electrolyte that formed a stable interfacial binding layer on lithium metal, promoting uniform nucleation and suppressing localized current concentration (Figs. 9b–9d).[89] Consequently, lithium deposited as nanoscale spherical particles rather than dendrites. *in situ* XRD and cryo-TEM analyses confirmed the preferential exposure of low-index crystal facets, indicating a controlled crystal growth. This system enabled stable cycling of Li symmetric cells for over 1200 h at 5 mA·cm^{-2} and achieved 95.5% capacity retention after 200 cycles at 1 C in Li||S cells.

While adhesion helps maintain interfacial contact, adaptive polymer electrolytes further address the continuous structural evolution that occurs during deformation and cycling. These systems are designed to dynamically reorganize their network structure or intermolecular interactions in response to mechanical stress, thereby preserving both mechanical integrity and interfacial compatibility. Yang *et al.* reported a three dimensional coordinated electrolyte, formed by crosslinking a boron centered lithium salt with PVDF-HFP.[90] In this electrolyte, conformational transitions of the boron centered units, together with electrostatic interactions from bis(benzene sulfonyl)imide, generated a dynamically reconfigurable network. This structure enabled Young's modulus of 1.4 GPa and elongation at break of 447.4%, indicating excellent mechanical adaptability. Meanwhile, the LiF-rich interphase improved interfacial stability and helped accommodate volume changes in high-energy cathodes such as

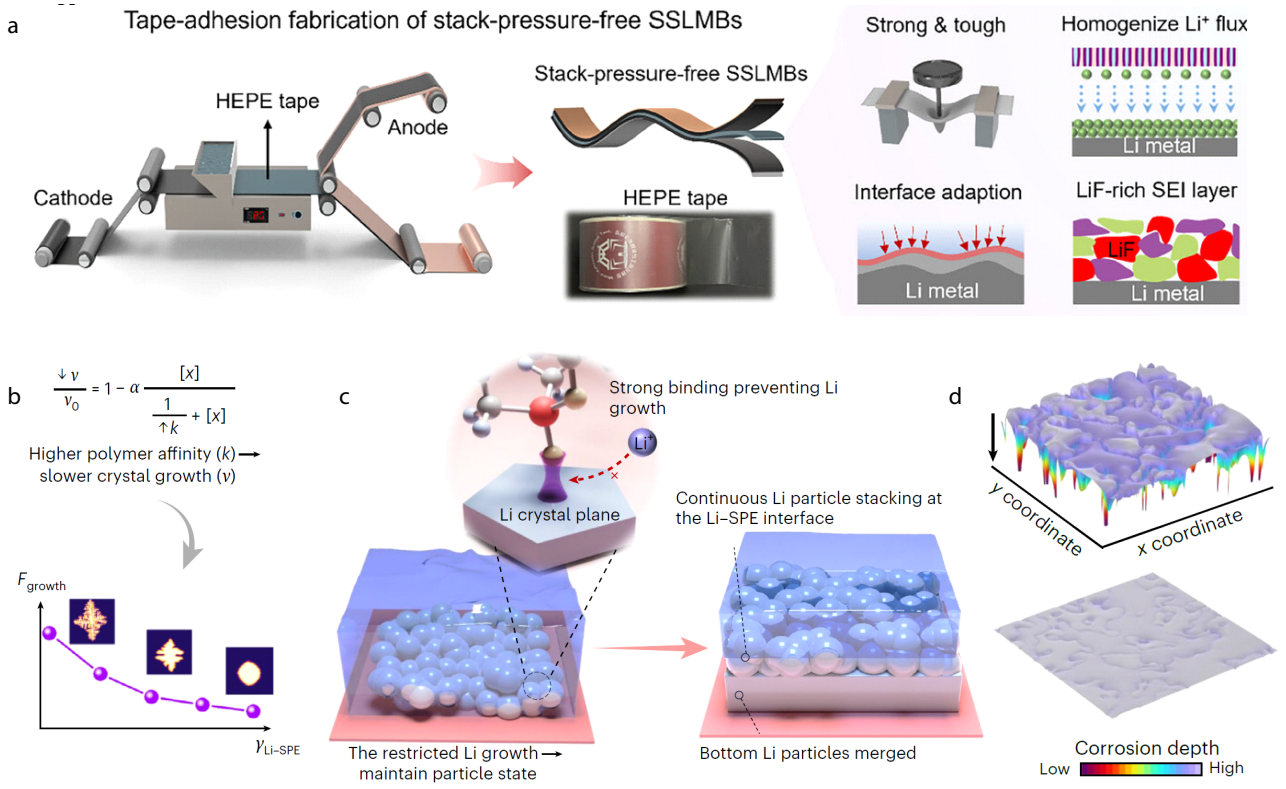

Fig. 9 (a) Tape-adhesion fabrication of stack-pressure-free solid-state lithium batteries and overview of the essential properties and functions of high-entropy polymer electrolyte in physico-electrochemically stabilizing the Li metal anode (Reproduced with permission from Ref. [88]; Copyright (2026), Wiley-VCH); (b) The Bliznakov–Chernov equation describing the relationship between a polymer's affinity (*k*) for the crystal surface and the rate of crystal growth; (c) Continuous lithium particle stacking deposition mode in the high-viscosity SPE; (d) Corrosion depth distribution at the anode surface under conventional SPE (top, incomplete contact interface) and viscous SPE (bottom, complete contact interface) (b–d: reproduced with permission from Ref. [89]; Copyright (2026), Springer Nature).

$LiNi_{0.8}Co_{0.1}Mn_{0.1}O_2$ (NCM811), thereby maintaining structural integrity and electrochemical performance under deformation.

To further address irreversible damage accumulated during long-term operation, self-healing polymer electrolytes introduce dynamic bonds that enable autonomous repair of structural defects. Chen *et al.* developed a self-healing electrolyte (PDDP) by incorporating dynamic disulfide bonds and hydrogen bonding interactions into a crosslinked polymer network.[91] These dynamic bonds allowed the electrolyte film to heal autonomously at room temperature without external stimuli, recover mechanical integrity within seconds, and sustain mechanical loads after prolonged healing. Electrochemically, Li||PDDP||LFP cells retained a discharge capacity of 137.6 $mAh{\cdot}g^{-1}$ after 300 cycles at 0.2 C with an average Coulombic efficiency of 99.9%. The healed electrolyte also nearly recovered its original ionic conductivity and cycling performance, confirming the effectiveness of dynamic bond mediated repair. Extending this concept to composite electrolytes, Jiang *et al.* developed PBHL@LLZTO@DDB by incorporating silane coupling agent (DDB)-modified LLZTO inorganic fillers into a polyurethane (PBHL) matrix *via* synergistic disulfide-bonding and hydrogen-bonding interactions.[92] This design improved filler-polymer compatibility while preserving efficient self-repair. As a result, Li symmetric cells operated stably for over 3300 h, and full cells using LFP and NCM811 cathodes both exhibited excellent cycling stability. Pouch cells also maintained safe operation after mechanical cutting, highlighting the value of self-healing electrolytes for flexible energy storage applications.

4.2 Safety-oriented Design of SPEs

Flexible batteries are expected to remain safe under both electrochemical operation and deformation related abuse, including bending, compression, puncture, and local overheating. These conditions may trigger polymer electrolyte decomposition, producing flammable small molecules and reactive radicals such as H· and OH·. The radicals can sustain combustion through chain reactions, while the released heat further accelerates polymer degradation and radical generation, increasing the risk of thermal runaway (Fig. 10a).[93] Therefore, flame retardant design is essential for achieving safe SPEs used in flexible batteries. Mechanistically, flame retardancy is mainly achieved through gas phase radical quenching, dilution of combustible species, and formation of protective char layers.[94] Based on these mechanisms, current strategies can be classified into flame retardant additive incorporation and intrinsically flame-retardant polymer design.

The incorporation of flame-retardant additives represents a direct and versatile route to enhance fire safety without fundamentally altering the polymer backbone. Halogen-containing additives, particularly brominated compounds, are widely used due to their high efficiency and low loading requirements. These materials primarily function through gas-phase radical quenching: upon heating, they decompose to generate halogen-containing species that capture H· and OH· radicals, thereby interrupting combustion chain reactions.[95]

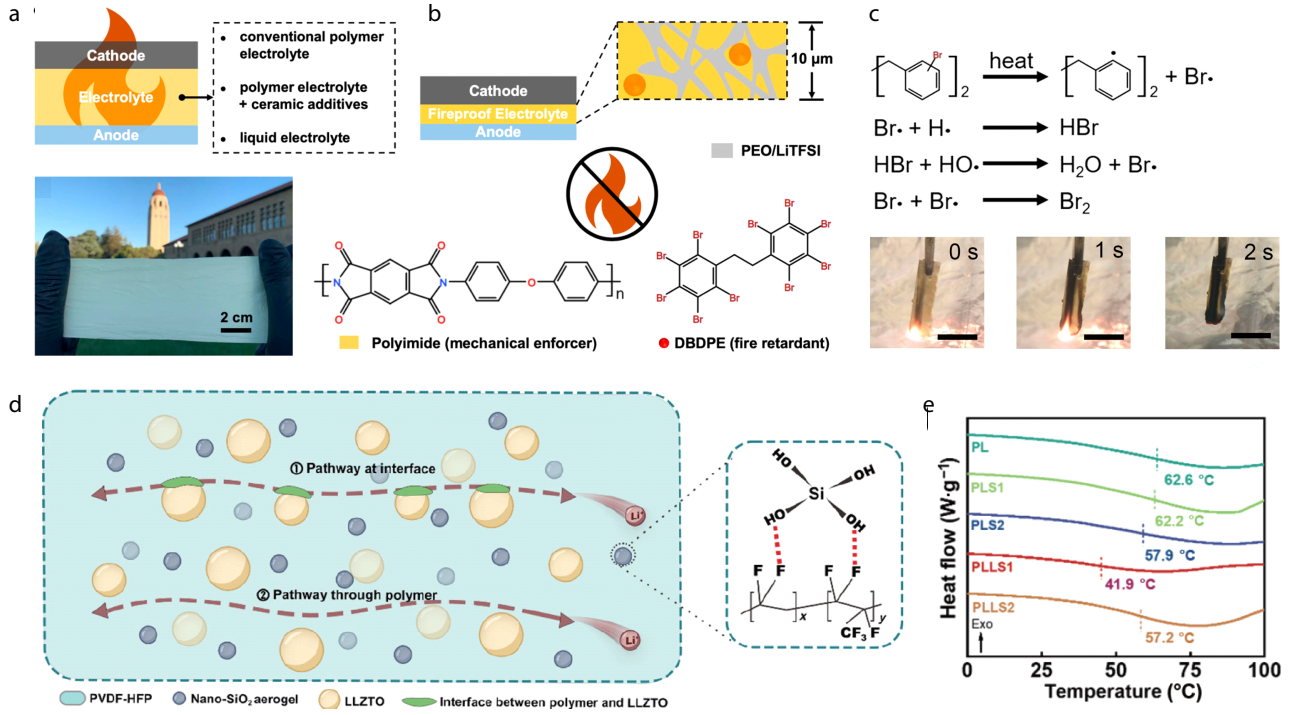

Fig. 10 (a) Conventional lithium-based batteries based on liquid and solid polymer-based electrolytes; (b) Design principles of the fireproof and lightweight polymer–polymer solid-state electrolyte and the photo image of a porous PI/DBDPE film; (c) The mechanism for the flame retardance effects of DBDPE and the flame test of PI/DBDPE/PEO/LiTFSI (a–c: reproduced with permission from Ref. [97]; Copyright (2020), American Chemical Society); (d) Schematic of Li^+ transport pathway in dual-filler reinforced PVDF-HFP based polymer electrolyte; (e) DSC curves of PL (pristine PVDF-HFP/LiTFSI), PLS1 (with 1 wt% SiO_2 aerogel), PLS2 (with 2 wt% SiO_2 aerogel), PLLS1 (with 5 wt% LLZTO + 1 wt% SiO_2 aerogel), and PLLS2 (with 5 wt% LLZTO + 2 wt% SiO_2 aerogel) (d, e: reproduced with permission from Ref. [100]; Copyright (2024), Springer Nature).

Based on this mechanism, Cui *et al.* introduced decabromodiphenyl ethane (DBDPE) into PI/PEO/LiTFSI system (Fig. 10b).[96] The resulting electrolyte exhibited excellent flame retardancy, with self-extinguishing times within 10 s (Fig. 10c). In addition, DBDPE preferentially decomposed at the NCM811 cathode to form a LiBr-rich interfacial layer and a uniform organic cathode electrolyte interphase (CEI), enhancing oxidative stability.[97] Consequently, Li||NCM811 cells achieved an average Coulombic efficiency of 99.7% at a cutoff voltage of 4.5 V, while Li||LFP cells using thin (10–25 μm) membranes delivered 131 $mAh \cdot g^{-1}$ at 1 C and maintained stable operation even under the flame exposure.

Despite their effectiveness, the possible generation of toxic gases and dense smoke from halogenated additives has encouraged the exploration of safer and more environmentally benign alternatives. In this regard, phosphorus-containing additives have attracted particular attention because they can suppress combustion through both gas phase radical quenching and condensed phase char formation. For instance, Zhang *et al.* incorporated triethyl phosphate (TEP) into a thermoplastic polyurethane/PAN-based polymer electrolyte, where TEP decomposed to generate PO· and HPO· radicals that quenched H· and OH· species in the gas phase, while simultaneously forming phosphorus-rich surface layers that catalyzed dehydration and crosslinking reactions.[98] The resulting char layer acted as an effective barrier to heat and oxygen transfer, enabling rapid self-extinguishing behavior within 5 s. Inorganic additives further expanded flame retardant design by combining gas dilution, radical suppression, and surface protection. Han *et al.* introduced NH_4PF_6@polyamide-6 into a PEO/LiTFSI matrix.[99] Upon thermal decomposition, NH_3 and HF were released to dilute combustible gases, while phosphorus-oxygen species suppressed radical reactions and formed protective surface layers. As a result, the electrolyte containing 3 wt% NH_4PF_6 resisted ignition even under direct flame exposure. Beyond chemically active inorganic additives, thermally stable inorganic fillers can also improve flame retardancy by reinforcing the polymer matrix and regulating ion transport. Along this direction, Fang *et al.* constructed a PVDF-HFP based composite electrolyte (PLLSx) using SiO_2 aerogel and LLZTO dual fillers.[100] The fillers reduced polymer crystallinity and promoted salt dissociation, while hydrogen bonding interactions between SiO_2 aerogel and PVDF-HFP enhanced structural stability (Figs. 10d and 10e). As a result, the PLLS1 membrane exhibited self-extinguishing behavior, with Li symmetric cells cycling stably for over 1500 h and Li||NCM811 cells maintaining stable performance over 200 cycles at 1 C with an average Coulombic efficiency above 98.93%.

Compared with additive based strategies, intrinsic flame retardant design covalently incorporates flame retardant units into the polymer framework, which can reduce additive migration and improve interfacial compatibility during long term cycling. Li *et al.* developed a flame-retardant SPE *via in situ* copolymerization of diethyl vinyl phosphate with methyl methacrylate and allyl diglycol carbonate, covalently embedding phosphate units into the polymer structure.[101] This covalent design mitigated side reactions associated with free phosphate esters while preserving efficient flame retardancy. As a result, Li||LCO cells using flame-retardant SPE retained 81.2% capacity after 230 cycles, whereas electrolytes containing free TEP showed rapid degradation. Microcalorimetry further revealed a reduced heat release rate, and thermogravimetric-infrared spectroscopy confirmed the continuous release of flame retardant species above 500 °C, indicating durable fire resistance. Along this direction, Chen *et al.* further incorporated triallyl phosphate and fluorinated methacrylate segments into a vinyl carbonate-based polymer matrix, improving flame retardancy, oxidative stability, and lithium metal compatibility, highlighting that flame retardant functionality introduced at either the additive or polymer level can effectively enhance the safety of SPEs for advanced battery systems.[102]

4.3 Environmental Adaptability-oriented Design of SPEs

Flexible batteries often operate under coupled mechanical and thermal fluctuations, requiring SPEs to maintain stable performance across variable temperature conditions. At low temperatures, restricted polymer segmental motion reduces ionic conductivity and increases interfacial polarization, while at elevated temperatures, polymer softening and interfacial side reactions can weaken structural integrity and accelerate performance decay. Therefore, wide temperature operation requires SPEs that can simultaneously maintain efficient ion transport, stable electrode-electrolyte interfaces, and mechanical robustness under thermally diverse conditions.

At low temperatures, reduced polymer segmental mobility slows ion transport, while sluggish Li^+ de-solvation and unstable SEI or CEI structures increase interfacial resistance, together causing severe polarization and rapid capacity decay.[103] Therefore, polymer electrolytes are typically designed by regulating both solvation structures and interfacial chemistry to enable low-temperature operation. Ma *et al.* developed a ternary anion electrolyte system based on lithium bis(fluorosulfonyl)imide (LiFSI), $AgBF_4$, and $LiNO_3$, in which an anion competitive coordination strategy weakened Li^+ solvation and regulated the *in situ* polymerization of 1,3-dioxolane (DOL).[104] This design formed a gradient interface composed of a silver-based lithiophilic layer and a LiF-rich dense SEI, improving both ion transport and interfacial stability (Figs. 11a and 11b). As a result, the electrolyte achieved a Li^+ transference number of 0.78 at −20 °C, enabling Li symmetric cells to operate for over 600 h at 10 $mA \cdot cm^{-2}$ and Li||LFP cells to retain 93.65% of initial capacity after 150 cycles at −20 °C. Using a related low temperature design principle, Li *et al.* reported an *in situ* polymerized solid electrolyte based on 1,3,5-trioxane (TXE), 2,2,2-trifluoro-*N*,*N*-dimethylacetamide (FDMA), fluoroethylene carbonate (FEC), and lithium difluoro(oxalate)borate (LiDFOB).[105] In this system, LiDFOB served as both initiator and lithium salt, while FDMA with a melting point of −42 °C improved low temperature fluidity. The electrolyte delivered an ionic conductivity of 0.22 $mS \cdot cm^{-1}$ and a Li^+ transference number of 0.8 at −20 °C. Meanwhile, the formation of a $Li_xBO_yF_z$/LiF bilayer SEI further stabilized the interface, allowing Li||NCM811 cells to deliver 92 $mAh \cdot g^{-1}$ at −30 °C and extending the operating temperature limit to −48.2 °C. These strategies are also valuable for flexible batteries, where stable ion transport and intimate electrode electrolyte contact need

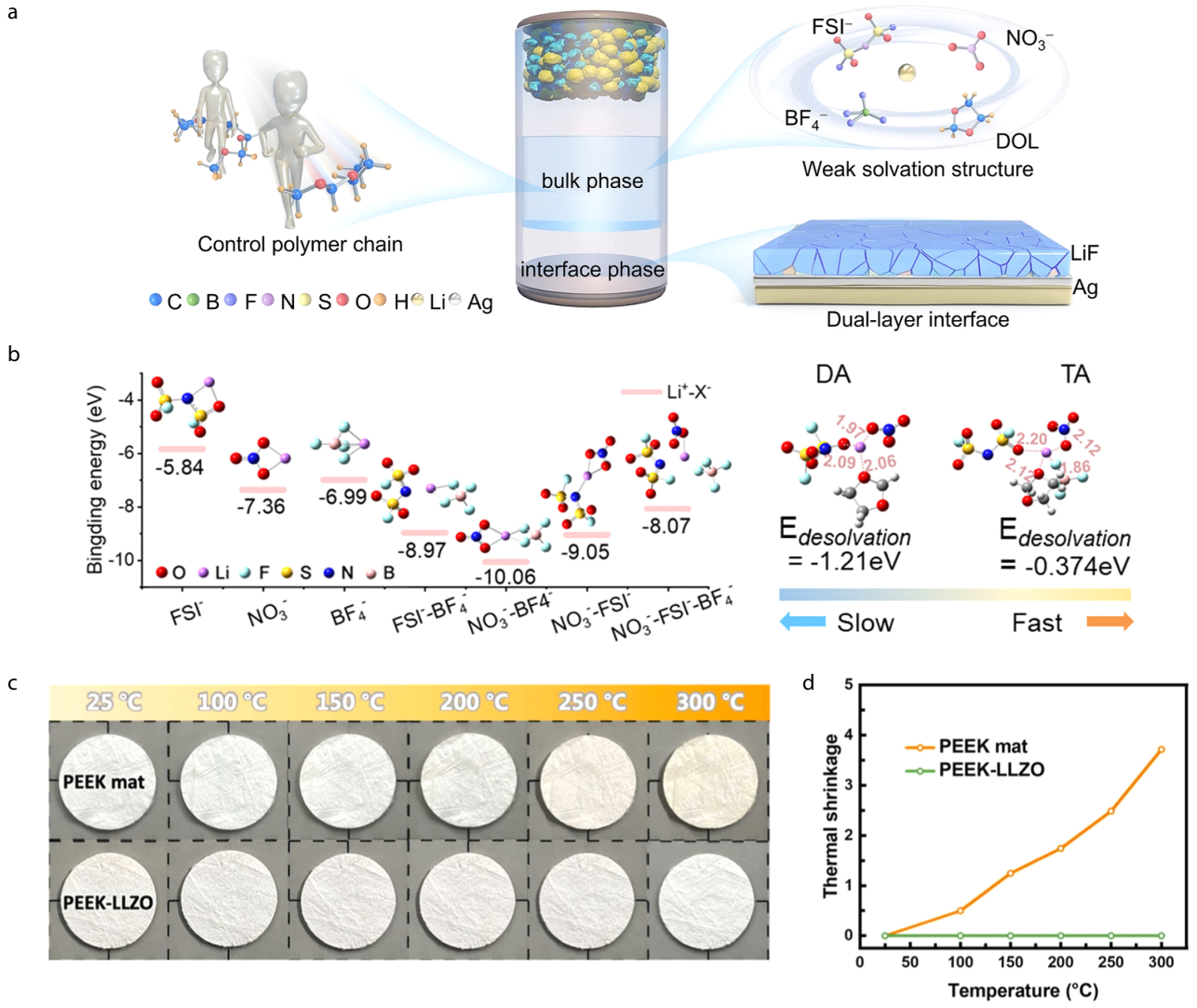

Fig. 11 (a) The design of *in situ* synthesized quasi-solid electrolyte with LiFSI, $AgBF_4$, $LiNO_3$, and DOL; (b) (Left) Binding energies of Li^+-anion-DOL solvation with single anion, dual anions, and ternary anions. (Right) Density functional theory simulations of the energy barrier for Li^+ desolvation in dual-anion (DA) and ternary-anion (TA) based SPEs (a, b: reproduced with permission from Ref. [104]; Copyright (2025), Wiley-VCH); (c) Photographs and (d) thermal shrinkage of PEEK and PEEK-LLZO mats after being treated at different temperatures (Reproduced with permission from Ref. [108]; Copyright (2025), Elsevier).

to be maintained under coupled thermal and mechanical conditions.

In contrast, high-temperature failure of SPEs is dominated by thermally induced structural degradation and intensified interfacial side reactions. Polymer softening or decomposition weakens mechanical integrity, while electrolyte oxidation and unstable SEI/CEI layers increase interfacial resistance and accelerate performance decay.[106] Addressing these issues requires the integration of thermally stable frameworks with robust interfacial regulation mechanisms. Zhu *et al.* developed an all-polymer electrolyte inspired by the "soft tissue-rigid skeleton" architecture of musculoskeletal systems.[107] This design combined thermally stable polyphosphazene as an ion-conducting phase with a crystalline PVDF-HFP framework that formed a three-dimensional reinforcing network through *in situ* microphase separation. The resulting electrolyte exhibited an electrochemical window of 5.66 V, achieved an ionic conductivity of 1.73×10^{-4} S·cm^{-1}, and maintained a mechanical strength of 0.32 MPa at 90 °C . Consequently, Li symmetric cells operated stably for 4500 h at 0.25 mA·cm^{-2}, while Li||LFP cells achieved 1000 stable cycles at 90 °C.

Thermally robust inorganic components can further extend the high temperature tolerance of polymer-based electrolytes. Dai *et al.* constructed a composite electrolyte by integrating a poly(ether ether ketone) (PEEK) nanofiber membrane with cubic phase $Li_7La_3Zr_2O_{12}$ (LLZO), achieving overall thermal stability above 300 °C (Figs. 11c and 11d).[108] X-ray photoelectron spectroscopy and atomic force microscopy analyses revealed smooth inorganic-rich SEI and CEI layers containing LiF, Li_3N, and Li_2O, which suppressed lithium dendrite growth and interfacial side reactions at high temperatures. Consequently, the electrolyte maintained an ionic conductivity of 2.40 mS·cm^{-1} even at 250 °C, and Li||LFP cells re-

tained 92.8% capacity after 50 cycles at 1 C, highlighting the potential of thermally stable composite frameworks for flexible batteries operating under coupled thermal and mechanical stress.

5 CONCLUSIONS AND PERSPECTIVES

In recent years, substantial efforts have been devoted to polymer solid state electrolytes for flexible solid-state batteries. This review organizes recent advances around three closely connected themes: polymer-based electrolytes design, fabrication/integration strategies, and application-oriented functions. The field has evolved from optimizing individual electrolyte properties toward designing SPEs as integrated electrochemical and mechanical components. Linear polymers, topological architectures, and composite systems have expanded the materials toolbox, while ex situ fabrication, *in situ* polymerization, and advanced manufacturing have improved processability and interfacial integration. In parallel, adhesive, adaptive, self-healing, flame retardant, and wide temperature electrolyte designs have begun to address the practical requirements of flexible and wearable energy storage.

Despite these advances, practical flexible solid-state batteries remain at an early stage, and several critical gaps need to be addressed. (i) The evaluation conditions used in many studies are still not sufficiently close to real flexible battery operation. Elevated temperature, low cathode loading, excess lithium, limited deformation cycles, or residual external pressure can obscure the true relevance of an electrolyte design. Standardized protocols that combine bending radius, repeated deformation, pressure free cycling, areal capacity, temperature window, and abuse tolerance are needed to establish meaningful benchmarks. (ii) Predictive structure-property relationships remain limited. In composite and multifunctional SPEs, polymer chains, fillers, salts, plasticizers, and interphases often act together, yet their individual roles are not always clearly distinguished. More quantitative links among polymer architecture, ion coordination, mechanical deformation, and interface evolution are required to move beyond empirical formulation optimization. (iii) The electrode-electrolyte interface remains a central bottleneck under deformation. Flexible batteries require low initial interfacial resistance as well as stable contact during bending, twisting, stretching, temperature fluctuation, and pressure free operation. Dynamic and durable interfaces that maintain continuous ion transport under coupled electrochemical and mechanical stress should therefore become a central design target. (iv) Ultrathin electrolyte construction is essential for high energy density, but thinner membranes are more susceptible to dendrite penetration, pinholes, tearing, and processing defects. Thickness reduction, mechanical reinforcement, dendrite resistance, and interfacial conformity should be optimized together at the device level, rather than treated as isolated membrane properties. (v) *In situ* and operando understanding under realistic flexible conditions is still insufficient. Techniques capable of tracking ion transport, phase evolution, stress distribution, and SEI or CEI formation during deformation and cycling will be important for identifying failure mechanisms.

Looking forward, future development should align materials discovery with these practical bottlenecks. (i) Refined interfacial engineering in composite electrolytes is needed to address filler aggregation, weak polymer filler compatibility, and discontinuous ion pathways. Surface functionalization, covalent bonding, and coordinative interactions provide useful routes to improve phase compatibility while preserving flexibility. (ii) *In situ* polymerization and other conformal processing strategies should be further explored for constructing ultrathin electrolytes with intimate electrode contact and improved defect tolerance. (iii) *In situ* and operando characterization should be expanded to conditions that combine electrochemical cycling, bending, twisting, pressure free operation, and temperature fluctuation. (iv) Data driven and high throughput approaches may accelerate the discovery of monomers, salts, fillers, plasticizers, and interfacial modifiers. Their predictive value will depend heavily on the comprehensiveness of the datasets, which should therefore include not only ionic conductivity and electrochemical stability, but also modulus, toughness, adhesion, deformation tolerance, interfacial resistance evolution, flame retardancy, wide temperature behavior, processability, and pressure free cycling. (v) Manufacturing and sustainability will also determine whether SPEs based flexible batteries can move beyond laboratory demonstrations. Many advanced electrolytes are still prepared as small area membranes or validated in coin cells, whereas practical flexible batteries require thin, uniform, large area electrolytes integrated with deformable electrodes and reliable encapsulation. Dry processing, continuous coating, *in situ* polymerization, and roll to roll compatible fabrication should be developed together with electrolyte chemistry to control membrane uniformity, filler dispersion, electrode infiltration, and interfacial adhesion. (vi) At the same time, lifecycle considerations should be incorporated earlier in electrolyte design, including solvent consumption, material toxicity, recyclability, and compatibility with battery recycling processes.

In summary, polymer solid state electrolytes provide a promising materials platform for flexible and wearable energy storage because of their softness, processability, and structural tunability. The next stage of the field should shift from optimizing isolated electrolyte metrics toward integrated design across polymer chemistry, electrode interfaces, device architecture, mechanical operation, safety, manufacturability, and sustainability. This coordinated approach is expected to accelerate the transition of flexible polymer solid state batteries from laboratory demonstrations to practical applications.

BIOGRAPHY

Meng Liao is an Assistant Professor in the Department of Macromolecular Science at Fudan University. He received his B.S. degree in Polymer Materials and Engineering from Sichuan University in 2016 and his Ph.D. degree in Polymer Chemistry and Physics from Fudan University in 2021 under the supervision of Professor Huisheng Peng. He then conducted postdoctoral research at The Pennsylvania State University and City University of Hong Kong. In 2025, he joined Fudan University and was selected for the National High-Level Young Talent Program. His research focuses on functional polymer materials for advanced electrochemical energy storage.

https://doi.org/10.1007/s10118-026-3799-y

Conflict of Interests

Hui-Sheng Peng is an editorial board member for *Chinese Journal of Polymer Science* and was not involved in the editorial review or the decision to publish this article. The authors declare no interest conflict.

ACKNOWLEDGMENTS

This work was financially supported by the National Natural Science Foundation of China (Nos. 22335003 and 22475051).

REFERENCES

1 Jiang, H.; Liao, M.; Chang, Y.; Zhang, K.; Jiang, Y.; Wang, B.; Peng, H. Design and application of fiber batteries. *Acta Polymerica Sinica (in Chinese)* **2023**, 54, 892–909.
2 Saifi, S.; Xiao, X.; Cheng, S.; Guo, H.; Zhang, J.; Müller-Buschbaum, P.; Zhou, G.; Xu, X.; Cheng, H. An ultraflexible energy harvesting-storage system for wearable applications. *Nat. Commun.* **2024**, *15*, 6546.
3 Shi, X.; Zuo, Y.; Zhai, P.; Shen, J.; Yang, Y.; Gao, Z.; Liao, M.; Wu, J.; Wang, J.; Xu, X.; Tong, Q.; Zhang, B.; Wang, B.; Sun, X.; Zhang, L.; Pei, Q.; Jin, D.; Chen, P.; Peng, H. Large-area display textiles integrated with functional systems. *Nature* **2021**, *591*, 240–245.
4 Hong, Y.; Jia, K.; Zhang, Y.; Li, Z.; Jia, J.; Chen, J.; Liang, Q.; Sun, H.; Gao, Q.; Zhou, D.; Li, R.; Dong, X.; Fan, X.; He, S. Energetic and durable all-polymer aqueous battery for sustainable, flexible power. *Nat. Commun.* **2024**, *15*, 9539.
5 Ding, S.; Saha, T.; Yin, L.; Liu, R.; Khan, M.; Chang, A.; Lee, H.; Zhao, H.; Liu, Y.; Nazemi, A.; Zhou, J.; Chen, C.; Li, Z.; Zhang, C.; Earney, S.; Tang, S.; Djassemi, O.; Chen, X.; Lin, M.; Sandhu, S.; Moon, J.; Moonla, C.; Nandhakumar, P.; Park, Y.; Mahato, K.; Xu, S.; Wang, J. A fingertip-wearable microgrid system for autonomous energy management and metabolic monitoring. *Nat. Electron.* **2024**, *7*, 788–799.
6 Hong, Y.; Cheng, X.; Liu, G.; Hong, D.; He, S.; Wang, B.; Sun, X.; Peng, H. One-step production of continuous supercapacitor fibers for a flexible power textile. *Chinese J. Polym. Sci.* **2019**, *37*, 737–743.
7 Ye, L.; Liao, M.; Zhang, K.; Zheng, M.; Jiang, Y.; Cheng, X.; Wang, C.; Xu, Q.; Tang, C.; Li, P.; Wen, Y.; Xu, Y.; Sun, X.; Chen, P.; Sun, H.; Gao, Y.; Zhang, Y.; Wang, B.; Lu, J.; Zhou, H.; Wang, Y.; Xia, Y.; Xu, X.; Peng, H. A rechargeable calcium–oxygen battery that operates at room temperature. *Nature* **2024**, *626*, 313–318.
8 Fu, J.; Wang, C.; Wang, S.; Reid, J.; Liang, J.; Luo, J.; Kim, J.; Zhao, Y.; Yang, X.; Zhao, F.; Li, W.; Fu, B.; Lin, X.; Hu, Y.; Su, Y.; Hao, X.; Gao, Y.; Zhang, S.; Wang, Z.; Liu, J.; Abdolvand, H.; Sham, T.; Mo, Y.; Sun, X. A cost-effective all-in-one halide material for all-solid-state batteries. *Nature* **2025**, *643*, 111–118.
9 Ye, L.; Wang, D.; Lu, Q.; Jhang, L.; Kou, R.; Pandey, A.; Lira, J.; Liao, M.; Wang, D. All-solid-state lithium-sulfur batteries of high cycling stability and rate capability enabled by a self-lithiated Sn-C interlayer. *Adv. Mater.* **2025**, *37*, 2407724.
10 Zhang, D.; Ren, Y.; Hu, Y.; Li, L.; Yan, F. Ionic liquid/poly (ionic liquid)-based semi-solid state electrolytes for lithium-ion batteries. *Chinese J. Polym. Sci.* **2020**, *38*, 506–513.
11 Xie, Y.; Feng, L.; Li, D.; Tang, Y.; Zhu, C.; Wang, M.; Xu, J. Novel

Graphical Abstract

Solid Polymer Electrolytes for Flexible Solid-State Batteries

Jia-Xin Li, Kun Zhang, Jia-Wei Zhao, Shi-Ze Gao, Chen Zhao, Bing-Jie Wang, Hui-Sheng Peng, and Meng Liao

Fudan University

Solid polymer electrolytes enable flexible solid-state batteries by integrating ion transport, mechanical adaptability, and interfacial stability. This review highlights solid polymer electrolyte design, composite strategies, fabrication methods, and application-oriented functions for deformation tolerance, safety, and environmental adaptability for flexible solid-state batteries.

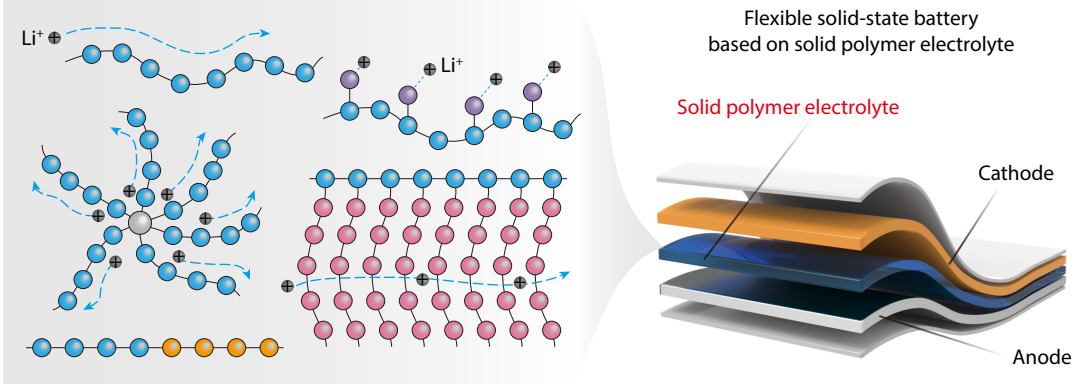

Chinese J. Polym. Sci., 2026 *https://doi.org/10.1007/s10118-026-3799-y*

quasi solid-state succinonitrile-based electrolyte with low-flammability for lithium-ion battery. *Chinese J. Polym. Sci.* **2023**, *41*, 1695–1705.
12 Doux, J.; Nguyen, H.; Tan, D.; Banerjee, A.; Wang, X.; Wu, E.; Jo, C.; Yang, H.; Meng, Y. Stack pressure considerations for room-temperature all-solid-state lithium metal batteries. *Adv. Energy Mater.* **2020**, *10*, 1903253.
13 Hu, X.; Zhang, Z.; Zhang, X.; Wang, Y.; Yang, X.; Wang, X.; Fayena-Greenstein, M.; Yehezkel, H.; Langford, S.; Zhou, D.; Li, B.; Wang, G.; Aurbach, D. External-pressure–electrochemistry coupling in solid-state lithium metal batteries. *Nat. Rev. Mater.* **2024**, *9*, 305–320.
14 Chen, Y.; Jang, J.; Oh, J.; Ham, S.; Yang, H.; Lee, D.; Vicencio, M.; Lee, J.; Tan, D.; Chouchane, M.; Cronk, A.; Song, M.; Yin, Y.; Qian, J.; Chen, Z.; Meng, Y. Enabling uniform and accurate control of cycling pressure for all-solid-state batteries. *Adv. Energy Mater.* **2024**, *14*, 2304327.
15 Pan, H.; Wang, L.; Shi, Y.; Sheng, C.; Yang, S.; He, P.; Zhou, H. A solid-state lithium-ion battery with micron-sized silicon anode operating free from external pressure. *Nat. Commun.* **2024**, *15*, 2263.
16 Liu, K.; Xie, Y.; Ding, T.; Guo, C.; Guo, P.; Liu, J.; Liu, X.; Shi, L.; Pan, Z.; Cai, X.; Wang, J.; Wang, Z.; Shi, G.; Yuan, S. High-strength ultrathin solid-state electrolyte with ion-rectifying honeycomb-like skeleton for lithium metal batteries free from external pressure. *Adv. Funct. Mater.* **2026**, *36*, e11558.
17 Fenton, D.; Parker, J.; Wright, P. Complexes of alkali metal ions with poly(ethylene oxide). *Polymer* **1973**, *14*, 589.
18 Du, A.; Lu, H.; Liu, S.; Chen, S.; Chen, Z.; Li, W.; Song, J.; Yang, Q.; Yang, C. Breaking the trade-off between ionic conductivity and mechanical strength in solid polymer electrolytes for high-performance solid lithium batteries. *Adv. Energy Mater.* **2024**, *14*, 2400808.
19 Lv, Q.; Li, L.; Zhang, X.; Wang, R.; Wen, N.; Xue, L.; Wang, H.; Shen, L.; Chen, D.; Ciucci, F.; Wang, J. Developing dynamic ion transport channels in polymer solid electrolytes for high-performance lithium metal batteries. *J. Am. Chem. Soc.* **2025**, *147*, 27611–27623.
20 Xi, G.; Xiao, M.; Wang, S.; Han, D.; Li, Y.; Meng, Y. Polymer-based solid electrolytes: material selection, design, and application. *Adv. Funct. Mater.* **2021**, *31*, 2007598.
21 Choudhury, S.; Stalin, S.; Vu, D.; Warren, A.; Deng, Y.; Biswal, P.; Archer, L. Solid-state polymer electrolytes for high-performance lithium metal batteries. *Nat. Commun.* **2019**, *10*, 4398.
22 Zhu, X.; Wang, K.; Xu, Y.; Zhang, G.; Li, S.; Li, C.; Zhang, X.; Sun, X.; Ge, X.; Ma, Y. Strategies to boost ionic conductivity and interface compatibility of inorganic-organic solid composite electrolytes. *Energy Storage Mater.* **2021**, *36*, 291–308.
23 Armand, M. The history of polymer electrolytes. *Solid State Ion.* **1994**, *69*, 309–319.
24 Wei, Y.; Liu, T.; Zhou, W.; Cheng, H.; Liu, X.; Kong, J.; Shen, Y.; Xu, H.; Huang, Y. Enabling all-solid-state Li metal batteries operated at 30 °C by molecular regulation of polymer electrolyte. *Adv. Energy Mater.* **2023**, *13*, 2203547.
25 Zhang, J.; Zhao, J.; Yue, L.; Wang, Q.; Chai, J.; Liu, Z.; Zhou, X.; Li, H.; Guo, Y.; Cui, G.; Chen, L. Safety-reinforced poly (propylene carbonate)-based all-solid-state polymer electrolyte for ambient-temperature solid polymer lithium batteries. *Adv. Energy Mater.* **2015**, *5*, 1501082.
26 Li, H.; Fan, Y.; Wu, G.; Qiang, Y.; Wang, S.; Kang, Z.; Du, J.; Tang, Z.; Wang, W.; Li, W.; Gao, Y. Decoupling ionic conductivity from structural rigidity constraints of solid polymer electrolytes through microphase separation regulation. *ACS Energy Lett.* **2025**, *10*, 6423–6431.
27 Nagaoka, K.; Naruse, H.; Shinohara, I.; Watanabe, M. High ionic conductivity in poly(dimethyl siloxane-co-ethylene oxide) dissolving lithium perchlorate. *J. Polym. Sci.* **1984**, *22*, 659–663.
28 Liu, C.; Jia, S.; Yang, T.; Liu, J.; Zhou, X.; Wang, Z.; Dong, H.; Shi, Z.; Zhang, Y.; Chen, Z. Scalable and ultrathin dual entangled network polymer electrolytes for safe solid-state sodium batteries. *Angew. Chem. Int. Ed.* **2025**, *64*, e202505938.
29 Ma, Y.; Wan, J.; Yang, Y.; Ye, Y.; Xiao, X.; Boyle, D.; Burke, W.; Huang, Z.; Chen, H.; Cui, Y.; Yu, Z.; Oyakhire, S.; Cui, Y. Scalable, ultrathin, and high-temperature-resistant solid polymer electrolytes for energy-dense lithium metal batteries. *Adv. Energy Mater.* **2022**, *12*, 2103720.
30 Yang, H.; Yan, J.; Gao, S.; Chen, X.; Wang, Y.; Huo, H.; Fu, C.; Du, C.; Zuo, P. An asymmetric functional gel polymer electrolyte enables superior interfacial compatibility for wide temperature lithium metal batteries. *Energy Environ. Sci.* **2025**, *18*, 9854–9864.
31 Zhang, Q.; Bian, T.; Wang, X.; Shi, R.; Zhao, Y. Unlocking mechanism of anion and cation interaction on ion conduction of polymer based electrolyte in metal batteries. *Angew. Chem. Int. Ed.* **2025**, *64*, e202415343.
32 Liu, F.; Wang, J.; Chen, W.; Yuan, M.; Wang, Q.; Ke, R.; Zhang, G.; Chang, J.; Wang, C.; Deng, Y.; Wang, J.; Shao, M. Polymer-ion interaction prompted quasi-solid electrolyte for room-temperature high-performance lithium-ion batteries. *Adv. Mater.* **2024**, *36*, 2409838.
33 Lian, Y.; Li, M.; Gao, Y.; Zhao, M.; Liu, J.; Xiao, L. An electrochemically stable polyester fabric-reinforced poly (methyl methacrylate) gel polymer electrolyte for solid-state lithium–oxygen batteries. *ACS Appl. Energy Mater.* **2023**, *6*, 11364–11375.
34 Li, Y.; Yuan, W.; Hu, Z.; Shen, Y.; Wu, G.; Cong, F.; Fu, X.; Lu, F.; Li, Y.; Liu, P.; Huang, Y.; Li, J. Constructing PVDF-based polymer electrolyte for lithium metal batteries by polymer-induced phase structure adjustment strategy. *Adv. Funct. Mater.* **2025**, *35*, 2424763.
35 Jie, J.; Liu, Y.; Cong, L.; Zhang, B.; Lu, W.; Zhang, X.; Liu, J.; Xie, H.; Sun, L. High-performance PVDF-HFP based gel polymer electrolyte with a safe solvent in Li metal polymer battery. *J. Energy Chem.* **2020**, *49*, 80–88.
36 Wang, T.; Zhong, L.; Xiao, M.; Han, D.; Wang, S.; Huang, Z.; Huang, S.; Sun, L.; Meng, Y. Block copolymer electrolytes for lithium metal batteries: Strategies to boost both ionic conductivity and mechanical strength. *Prog. Polym. Sci.* **2023**, *146*, 101743.
37 Su, G.; Zhang, Z.; Xiao, M.; Wang, S.; Huang, S.; Guo, H.; Han, D.; Meng, Y. Boosting electrochemical performance by regulating rigid-flexible microphase separation of multiblock copolymers. *Chem. Eng. J.* **2024**, *500*, 157050.
38 Wang, H.; Li, X.; Zeng, Q.; Li, Z.; Liu, Y.; Guan, J.; Jiang, Y.; Chen, L.; Cao, Y.; Li, R.; Wang, A.; Wang, Z.; Zhang, L. A novel hyperbranched polyurethane solid electrolyte for room temperature ultra-long cycling lithium-ion batteries. *Energy Storage Mater.* **2024**, *66*, 103188.
39 Su, Y.; Rong, X.; Li, H.; Huang, X.; Chen, L.; Liu, B.; Hu, Y. High-entropy microdomain interlocking polymer electrolytes for advanced all-solid-state battery chemistries. *Adv. Mater.* **2023**, *35*, 2209402.
40 Ye, L.; Wei, J.; Yuan, S.; Wang, J.; Wang, Y.; Cao, C.; Tan, F.; Shen, H.; Qin, R.; Li, Y.; Chen, X. High-entropy polymeric electrolytes facilitating ion conduction and interfacial desolvation in low-temperature zinc batteries. *J. Am. Chem. Soc.* **2026**, *148*, 7605–7613.
41 Hao, S.; Liang, S.; Sewell, C.; Li, Z.; Zhu, C.; Xu, J.; Lin, Z. Lithium-conducting branched polymers: New paradigm of solid-state electrolytes for batteries. *Nano Lett.* **2021**, *21*, 7435–7447.

42 Fish, D.; Khan, I.; Wu, E.; Smid, J. Polymer electrolyte complexes of $LiClO_4$ and comb polymers of siloxane with oligo-oxyethylene side chains. *Br. Polym. J.* **1988**, *20*, 281–288.

43 Han, S.; Arbeli, A.; Harrison, K.; Orchanian, N.; Lei, W.; Louie, S.; Jiang, Q.; Kumar, Z.; Dolinski, N.; Kaufman, L.; Marbella, L.; Nuckolls, C. Ion-conductive wires form high-performance all-solid-state polymer electrolytes. *J. Am. Chem. Soc.* **2026**, *148*, 9413–9420.

44 Xu, H.; Zhang, J.; Zhang, H.; Long, J.; Xu, L.; Mai, L. *In situ* topological interphases boosting stable solid-state lithium metal batteries. *Adv. Energy Mater.* **2023**, *13*, 2204411.

45 Chen, H.; Zhang, Z.; Qin, H.; Zhang, B.; Wang, D.; Ming, L.; Ou, X. Topological polymer electrolyte design with dual confinements for long-life quasi-solid-state lithium-sulfur batteries. *Adv. Funct. Mater.* **2025**, *35*, 2506355.

46 He, Y.; Yang, S.; Liu, C.; Ouyang, Y.; Li, Y.; Zhu, H.; Yao, Y.; Yang, H.; Rui, X.; Yu, Y. Composite polymer solid electrolytes for all-solid-state sodium batteries. *Small Methods* **2025**, *9*, 2402220.

47 Chen, S.; Huang, B.; Song, L.; Wang, Z.; Du, P.; Xiong, J.; Zhu, H.; Guo, Y. High ionic conductive, mechanical robust solid polymer composite electrolyte achieved by succinonitrile and polytetrafluoroethylene porous fibrous membrane for lithium metal batteries. *Chinese J. Polym. Sci.* **2026**, *44*, 352–360.

48 Pan, J.; Peng, H.; Yan, Y.; Bai, Y.; Yang, J.; Wang, N.; Dou, S.; Huang, F. Solid-state batteries designed with high ion conductive composite polymer electrolyte and silicon anode. *Energy Storage Mater.* **2021**, *43*, 165–171.

49 Fan, P.; Liu, H.; Marosz, V.; Samuels, N.; Suib, S.; Sun, L.; Liao, L. High performance composite polymer electrolytes for lithium-ion batteries. *Adv. Funct. Mater.* **2021**, *31*, 2101380.

50 Banerjee, A.; Wang, X.; Fang, C.; Wu, E.; Meng, Y. Interfaces and interphases in all-solid-state batteries with inorganic solid electrolytes. *Chem. Rev.* **2020**, *120*, 6878–6933.

51 Liu, S.; Liu, W.; Ba, D.; Zhao, Y.; Ye, Y.; Li, Y.; Liu, J. Filler-integrated composite polymer electrolyte for solid-state lithium batteries. *Adv. Mater.* **2023**, *35*, 2110423.

52 Ma, T.; Fu, B.; Feng, H.; Li, Y.; Zhai, Y.; Tian, Y.; Li, Z.; Su, Z. Porous aromatic frameworks filler with anion-constrained centers in composite polymer electrolyte for lithium-ion batteries. *Angew. Chem. Int. Ed.* **2025**, *64*, e202501412.

53 Wang, W.; Jia, M.; Bi, Z.; Guo, X. Porous g-C_3N_4 microspheres wrapped by garnet nanoparticles enable solid composite electrolytes with improved ionic conduction and interfacial stability. *Adv. Funct. Mater.* **2025**, *35*, 2419182.

54 Lan, X.; Li, Z.; Zhao, C.; Li, Z.; Zeng, Y.; Liu, Y.; Liu, Q.; Li, X.; Zhang, L.; Chen, Z.; Feng, X.; Wang, J.; Ding, F.; Hu, R.; Peng, J.; Cheng, H. Superionic composite electrolytes with continuously perpendicular-aligned pathways for pressure-less all-solid-state lithium batteries. *Nat. Nanotechnol.* **2026**, *21*, 388–396.

55 Shen, J.; Tian, W.; Liu, S.; Pan, H.; Yang, C.; Quan, H.; Zhu, S. Halogen-bonding nanoarchitectonics in supramolecular plasticizers for breaking the trade-off between ion transport and mechanical strength of polymer electrolytes for high-voltage Li-metal batteries. *ACS Nano* **2024**, *18*, 30716–30727.

56 Ren, Y.; Chen, S.; Odziomek, M.; Guo, J.; Xu, P.; Xie, H.; Tian, Z.; Antonietti, M.; Liu, T. Mixing functionality in polymer electrolytes: a new horizon for achieving high-performance all-solid-state lithium metal batteries. *Angew. Chem. Int. Ed.* **2025**, *64*, e202422169.

57 Qiu, H.; Yang, Y.; Liu, C.; Yao, Y.; Wu, Z.; He, S.; Pan, H.; Rui, X.; Yu, Y. Dual-conduction polymer electrolyte and stable interphase engineering for room-/subzero-temperature, long-cycling all-solid-state sodium batteries. *Adv. Mater.* **2026**, *38*, e19121.

58 Guo, M.; Gao, S.; Wang, Y.; Liu, K.; Zhao, J.; Zhang, Z.; Li, Y.; Li, C.; Zhang, L. Stabilization the electrode/electrolyte interphase by reconstructing the solvation structure of eutectic-based polymer electrolyte. *Adv. Funct. Mater.* **2026**, *36*, e09739.

59 Wang, S.; Wu, C.; Li, C.; Wu, X.; Liu, C.; Cui, H.; Wu, W.; Li, L.; Lai, W. Eutectic-based polymer electrolyte with high ionic conductivity by regulating solvation for solid-state lithium metal batteries. *Angew. Chem. Int. Ed.* **2026,** doi: 10.1002/anie.7290677.

60 Liu, Y.; Ye, C.; Chen, Y.; Cheng, Y.; Ding, Y.; Tang, S. Double-donor and anion-π polymer electrolytes for fast Li^+ conduction in lithium metal batteries. *Angew. Chem. Int. Ed.* **2025**, *64*, e202516098.

61 Wang, H.; Yang, J.; Xu, X.; Geng, J.; Lin, X.; Xu, H.; Huang, Y. Competitive ion coordination in gel polymer electrolytes enables decoupling of mechanical strength and ionic conductivity. *Adv. Mater.* **2025**, *37*, e04625.

62 Lee, M.; Han, J.; Lee, K.; Lee, Y.; Kim, B.; Jung, K.; Kim, B.; Lee, S. Elastomeric electrolytes for high-energy solid-state lithium batteries. *Nature* **2022**, *601*, 217–222.

63 Li, B.; Wang, C.; Yu, R.; Han, J.; Jiang, S.; Zhang, C.; He, S. Recent progress on metal–organic framework/polymer composite electrolytes for solid-state lithium metal batteries: ion transport regulation and interface engineering. *Energy Environ. Sci.* **2024**, *17*, 1854–1884.

64 Hong, Z.; Li, P.; Zou, Q.; Gu, L.; Wang, J.; Deng, L.; Wang, C.; Zhang, Y.; Li, M.; Chen, J.; Si, R.; Yang, C. Metal organic framework (MOF-808) incorporated composite polymer electrolyte for stable all-solid-state lithium batteries. *ACS Appl. Energy Mater.* **2024**, *7*, 11967–11976.

65 Deng, S.; Yu, H.; Shang, X.; Hao, Q.; Tian, F.; Ge, Z.; Li, Z. A Self-crosslinking MOF-based electrolyte enabling stable and selective Li^+ conduction in solid-state lithium batteries. *Adv. Funct. Mater.* **2026**, *36*, e74779.

66 Sasieta-Barrutia, E.; Blanco, J.; Liendo, G.; López del Amo, J.; Armand, M.; Otaegui, L.; Morant-Miñana, M.; Villaverde, A. Solid electrolyte manufacturing methods and its effect on SSB performance. *Chem. Eng. J.* **2024**, *501*, 157391.

67 Yu, R.; Ma, Y.; Zhang, N.; Qiu, T.; Jiang, Q.; Zhu, G. Confined polymer electrolyte synthesis in porous frameworks for cold-climate zinc-ion batteries. *Adv. Mater.* **2025**, *37*, e11029.

68 Liao, M.; Wang, C.; Hong, Y.; Zhang, Y.; Cheng, X.; Sun, H.; Huang, X.; Ye, L.; Wu, J.; Shi, X.; Kang, X.; Zhou, X.; Wang, J.; Li, P.; Sun, X.; Chen, P.; Wang, B.; Wang, Y.; Xia, Y.; Cheng, Y.; Peng, H. Industrial scale production of fibre batteries by a solution-extrusion method. *Nat. Nanotechnol.* **2022**, *17*, 372–377.

69 Zhang, X.; Liu, T.; Zhang, S.; Huang, X.; Xu, B.; Lin, Y.; Xu, B.; Li, L.; Nan, C.; Shen, Y. Synergistic coupling between $Li_{6.75}La_3Zr_{1.75}Ta_{0.25}O_{12}$ and poly(vinylidene fluoride) induces high ionic conductivity, mechanical strength, and thermal stability of solid composite electrolytes. *J. Am. Chem. Soc.* **2017**, *139*, 13779–13785.

70 Yao, S.; Kalami, S.; Nam, S.; Goodenough, J.; Khani, H. Development of an Electrophoretic deposition method for the *in situ* fabrication of ultra-thin composite-polymer electrolytes for solid-state lithium-metal batteries. *Small* **2023**, *19*, 2208252.

71 Zheng, G.; Chen, Y.; Chen, R.; Li, X.; Chen, Z.; Zeng, Z.; Yan, H. Three-dimensional flame-retardant quasi-solid composite electrolyte with a fiber structure formed using the coaxial electrospinning to suppress lithium dendrite growth. *Chem. Eng. J.* **2025**, *518*, 164616.

72 Zhang, D.; Liu, Y.; Yang, S.; Zhu, J.; Hong, H.; Li, S.; Xiong, Q.; Huang, Z.; Wang, S.; Liu, J.; Zhi, C. Inhibiting residual solvent induced side reactions in vinylidene fluoride-based polymer electrolytes enables ultra-stable solid-state lithium metal batteries. *Adv. Mater.* **2024**, *36*, 2401549.

73 Whiteley, J.; Taynton, P.; Zhang, W.; Lee, S. Ultra-thin solid-state Li-ion electrolyte membrane facilitated by a self-healing

polymer matrix. *Adv. Mater.* **2015**, *27*, 6922–6927.
74 Zhao, L.; Hou, M.; Ren, K.; Yang, D.; Li, F.; Yang, X.; Zhou, Y.; Zhang, D.; Liu, S.; Lei, Y.; Liang, F. Hot-pressing enhances mechanical strength of PEO solid polymer electrolyte for all-solid-state sodium metal batteries. *Small Methods* **2024**, *8*, 2301579.
75 Song, J.; Shang, W.; Zhou, W.; Li, J.; Wu, X.; Li, W.; Zhang, R.; Liu, S. From issues to solutions: 3D printing for overcoming challenges in liquid-and solid-state batteries. *Energy Storage Mater.* **2025**, *79*, 104342.
76 Han, T.; Cui, Z.; Kuang, W.; Cai, Y.; Sun, J.; Li, Y. Ferroelectric nanofiber reinforced electrolyte empowers fully 3D-printed solid-state sodium-ion batteries. *Adv. Funct. Mater.* **2026**, *36*, e13625.
77 Yang, F.; Shen, Y.; Zhang, Z.; Ruan, W.; Rong, M.; Zhang, M. Ultra-long life solid-state lithium metal batteries enabled by 3D-printing of integrated porous cathode/composite polymer electrolyte with dynamic covalent bonds. *Adv. Mater.* **2025**, *37*, e09057.
78 Liu, Q.; Wang, L.; He, X. Toward practical solid-state polymer lithium batteries by *in situ* polymerization process: a review. *Adv. Energy Mater.* **2023**, *13*, 2300798.
79 Li, P.; Wang, S.; Hao, J.; Wang, X.; Hao, S.; Lu, Y.; Li, H.; Zhou, W.; Li, Y. Efficiencies of various *in situ* polymerizations of liquid electrolytes and the practical implications for quasi solid-state batteries. *Angew. Chem. Int. Ed.* **2023**, *62*, e202309613.
80 Nair, J.; Shaji, I.; Ehteshami, N.; Thum, A.; Diddens, D.; Heuer, A.; Winter, M. Solid polymer electrolytes for lithium metal battery *via* thermally induced cationic ring-opening polymerization (CROP) with an insight into the reaction mechanism. *Chem. Mater.* **2019**, *31*, 3118–3133.
81 Huang, X.; Zhao, C.; Kong, W.; Yao, N.; Shuang, Z.; Xu, P.; Sun, S.; Lu, Y.; Huang, W.; Li, J.; Shen, L.; Chen, X.; Huang, J.; Archer, L.; Zhang, Q. Tailoring polymer electrolyte solvation for 600 Wh kg^{-1} lithium batteries. *Nature* **2025**, *646*, 343–350.
82 Wen, P.; Zhao, Y.; Wang, Z.; Lin, J.; Chen, M.; Lin, X. Solvent-free synthesis of the polymer electrolyte *via* photo-controlled radical polymerization: toward ultrafast in-built fabrication of solid-state batteries under visible light. *ACS Appl. Mater. Interfaces* **2021**, *13*, 8426–8434.
83 He, L.; Ye, H.; Sun, Q.; Tieu, A.; Lu, L.; Liu, Z.; Adams, S. *in situ* curing enables high performance all-solid-state lithium metal batteries based on ultrathin-layer solid electrolytes. *Energy Storage Mater.* **2023**, *60*, 102838.
84 Zhu, J.; Ma, B.; Zhong, C.; Wang, Z.; Tian, C.; Weng, S.; Li, S.; Cao, M.; Wang, Z.; Li, Y.; Li, H.; Cheng, T.; Wang, X. *In situ* electrochemical polymerization enabling high-performance quasi-solid-state batteries. *Adv. Energy Mater.* **2026**, *16*, e04413.
85 Lu, C.; Jiang, H.; Cheng, X.; He, J.; Long, Y.; Chang, Y.; Gong, X.; Zhang, K.; Li, J.; Zhu, Z.; Wu, J.; Wang, J.; Zheng, Y.; Shi, X.; Ye, L.; Liao, M.; Sun, X.; Wang, B.; Chen, P.; Wang, Y.; Peng, H. High-performance fibre battery with polymer gel electrolyte. *Nature* **2024**, *629*, 86–91.
86 Yang, L.; Wang, Z.; Feng, Y.; Tan, R.; Zuo, Y.; Gao, R.; Zhao, Y.; Han, L.; Wang, Z.; Pan, F. Flexible composite solid electrolyte facilitating highly stable "soft contacting" Li-electrolyte interface for solid state lithium-ion batteries. *Adv. Energy Mater.* **2017**, *7*, 1701437.
87 Pan, J.; Zhao, P.; Wang, N.; Huang, F.; Dou, S. Research progress in stable interfacial constructions between composite polymer electrolytes and electrodes. *Energy Environ. Sci.* **2022**, *15*, 2753–2775.
88 Chen, Y.; Jing, L.; Cai, W.; Cao, Z.; Ma, C.; Li, R.; Wu, Y.; Lv, S.; Zhai, Y.; Yang, W.; Wang, Y.; Fu, X. A Gradient nanodomain high-entropy polymer electrolyte tape for pressure-free solid-state lithium batteries. *Adv. Mater.* **2026**, *38*, e20657.
89 Li, C.; Lu, G.; Wu, X.; Zhang, M.; Wu, X.; Piao, Z.; Xiao, X.; Han, Z.; Zhong, X.; Qiao, Q.; Chen, B.; Wang, Y.; Zhou, G.; Cheng, H. Confining lithium in a continuous nucleation state for dendrite-free solid-state lithium metal batteries. *Nat. Synth.* **2026**, doi: 10.1038/s44160-026-01010-x.
90 Yang, Z.; Ye, Y.; Meng, N.; Lian, F. Adaptive 3D cross-linked single-ion conducting polymer electrolytes enable powerful interface for solid state batteries. *Angew. Chem. Int. Ed.* **2025**, *64*, e202505232.
91 Chen, K.; Sun, Y.; Zhang, X.; Liu, J.; Xie, H. A self-healing and nonflammable cross-linked network polymer electrolyte with the combination of hydrogen bonds and dynamic disulfide bonds for lithium metal batteries. *Energy Environ. Mater.* **2023**, *6*, e12568.
92 Jiang, Y.; Chen, K.; He, J.; Sun, Y.; Zhang, X.; Yang, X.; Xie, H.; Liu, J. A self-healing composite solid electrolyte with dynamic three-dimensional inorganic/organic hybrid network for flexible all-solid-state lithium metal batteries. *Colloid Interface Sci.* **2025**, *678*, 200–209.
93 Zhang, M.; Chen, Y.; Zheng, Y.; Shao, A.; Zhang, Y.; Zhang, C.; Zhou, Z.; Li, X.; Cheng, Y.; Gou, W.; Wang, M.; Zhan, Q.; Yu, M.; Yang, C.; Yang, R.; Wang, H.; Ahn, J.; Ma, Y. A thermally-activated molecular "firewall" composite solid electrolyte for inherently safe lithium metal batteries. *Adv. Funct. Mater.* **2026**, doi: 10.1002/adfm.75300.
94 Ma, X.; Lu, Y.; Ou, Y.; Yan, S.; Hou, W.; Zhou, P.; Liu, K. Strategies for flame-retardant polymer electrolytes for safe lithium-based batteries. *Nano Res.* **2024**, *17*, 8754–8771.
95 Altarawneh, M.; Saeed, A.; Al-Harahsheh, M.; Dlugogorski, B. Thermal decomposition of brominated flame retardants (BFRs): products and mechanisms. *Prog. Energy Combust. Sci.* **2019**, *70*, 212–259.
96 Cui, Y.; Wan, J.; Ye, Y.; Liu, K.; Chou, L.; Cui, Y. A fireproof, lightweight, polymer–polymer solid-state electrolyte for safe lithium batteries. *Nano Lett.* **2020**, *20*, 1686–1692.
97 Zhou, H.; Yan, S.; Li, J.; Dong, H.; Zhou, P.; Wan, L.; Chen, X.; Zhang, W.; Xia, Y.; Wang, P.; Wang, B.; Liu, K. Lithium bromide-induced organic-rich cathode/electrolyte interphase for high-voltage and flame-retardant all-solid-state lithium batteries. *ACS Appl. Mater. Interfaces* **2022**, *14*, 24469–24479.
98 Zhang, Z.; Zhao, T.; Huang, S.; Wang, S.; Han, D.; Guo, H.; Xiao, M.; Meng, Y. Flame retardant polyurethane-based semi-interpenetrating network electrolyte with continuous ion channel for high-voltage lithium-metal batteries. *Adv. Energy Mater.* **2025**, *15*, 2403678.
99 Han, L.; Liu, Y.; Liao, C.; Zhao, Y.; Cao, Y.; Kan, Y.; Zhu, J.; Hu, Y. Noncombustible 7 μm-thick solid polymer electrolyte for highly energy density solid state lithium batteries. *Nano Energy* **2023**, *112*, 108448.
100 Fang, C.; Huang, K.; Zhao, J.; Tian, S.; Dou, H.; Zhang, X. Dual-filler reinforced PVDF-HFP based polymer electrolyte enabling high-safety design of lithium metal batteries. *Nano Res.* **2024**, *17*, 5251–5260.
101 Li, Z.; Zhu, S.; Gao, S.; He, Y.; Ding, H.; Yang, D.; Yang, H.; Cao, P. Fireproof solid polymer electrolyte with chemically bonded phosphorus toward stable and safe lithium-metal battery. *Adv. Funct. Mater.* **2024**, *34*, 2409836.
102 Chen, J.; He, C.; Peng, X.; Li, J.; Xu, X.; Zhou, Y.; Shen, J.; Sun, J.; Li, Y.; Zhao, T. Puzzle-like molecular assembly of non-flammable solid-state polymer electrolytes for safe and high-voltage lithium metal batteries. *Nat. Commun.* **2025**, *16*, 8494.
103 Qu, Y.; Su, C.; Wang, L.; Li, B.; Jiang, W.; Li, R.; Pei, M.; Song, W.; Zhuo, S.; Jin, X.; Liu, D.; Jian, X.; Hu, F. Interface engineered electrolyte design strategy for ultralong-cycle solid-state

lithium batteries over wide temperature range. *Angew. Chem. Int. Ed.* **2025**, *64*, e202506731.
104 Ma, J.; Zhu, Y.; Wang, H.; Zhang, Y.; Wu, Q.; Qin, Z.; Zhang, J.; Liu, B.; Huang, D.; Ren, Y.; Nan, C.; Wang, X. Tuning anion chemistry to enhance bulk and interfacial stability in low-temperature lithium metal batteries. *Adv. Energy Mater.* **2025**, *15*, 2500631.
105 Li, Z.; Yu, R.; Weng, S.; Zhang, Q.; Wang, X.; Guo, X. Tailoring polymer electrolyte ionic conductivity for production of low-temperature operating quasi-all-solid-state lithium metal batteries. *Nat. Commun.* **2023**, *14*, 482.
106 Chang, G.; Zhao, H.; Cui, B.; Zhang, H.; Li, S.; Zhang, L.; Li, Z.; Qiu, J. Local thermal strain regulated solid electrolyte interphase with advanced high-temperature tolerance. *J. Am. Chem. Soc.* **2026**, doi: 10.1021/jacs.6c02582.
107 Zhu, G.; Zhang, Q.; Zhang, Y.; Wang, X.; Wu, G.; Wang, Y. Soft-hard synergistic solid all-polymer electrolyte inspired by musculoskeletal structure for high-temperature lithium metal batteries. *Adv. Funct. Mater.* **2025**, *35*, 2503481.
108 Dai, X.; Zhou, K.; Zhang, L.; Wu, T.; Ye, H.; Cao, X.; Han, Y.; Huang, G.; Xu, S. Polymer-based solid electrolyte with ultra thermostability exceeding 300 °C for high-temperature lithium-ion batteries in oil drilling industries. *Nano Energy* **2025**, *133*, 110475.